HOST UNIVERSITY: Ghent University

FACULTY: Faculty of Engineering

DEPARTMENT: Department of Flow, Heat and Combustion

Academic Year 2012-2013

COMBINING VOLUME SENSORS WITH MULTI-MODAL VIDEO ANALYSIS FOR FIRE DETECTION AND FORECASTING

Luis Alejandro Gonzalez Avila

Promoter: Bart Merci

Co-Promoter: Steven Verstockt

Master thesis submitted in the Erasmus Mundus Study Program

International Master of Science in Fire Safety Engineering

DISCLAIMER

This thesis is submitted in partial fulfillment of the requirements for the degree of *The International Master of Science in Fire Safety Engineering (IMFSE)*. This thesis has never been submitted for any degree or examination to any other University/program. The author(s) declare(s) that this thesis is original work except where stated. This declaration constitutes an assertion that full and accurate references and citations have been included for all material, directly included and indirectly contributing to the thesis. The author(s) gives (give) permission to make this master thesis available for consultation and to copy parts of this master thesis for personal use. In the case of any other use, the limitations of the copyright have to be respected, in particular with regard to the obligation to state expressly the source when quoting results from this master thesis. The thesis supervisor must be informed when data or results are used.

April 28th, 2013

Acknowledgements

Working in this thesis was an awesome experience, and it was mainly because of the help, company, advice and feedback of Professor Bart Merci and Dr. Steven Verstockt. Thank you both for promoting this innovative, interesting topic and for all your support during the months of work on it. The illustrating experiments carried out within the context of this work would not have been possible without the help of Mr. John De Blonde from Xtralis and Mr. Bart Sette and Mr. Patrick Claeys from WarringtonFire Gent. Also, my friends and thesis-mates from Gent made the months of work something more pleasant. Thanks Hélène, Josh and Victor for all the meals, all the talks, and all the support.

This book is not only the report of a thesis. It is the end of a fantastic experience that was being a student of the Erasmus Mundus International Master of Science in Fire Safety Engineering. Thanks everyone who made part of my learning and growing as a person the two years of my studies. Thanks to my parents and sister for their support. Thanks to the awesome friends I made in this program, Évi, Hélène, Beto, John. Thanks to all of my classmates because I am sure I learned something from each one of you. This moment is very exciting; I actually am a fire safety engineer!

Abstract

Insufficient lighting, steam, and dust, among others, lead to nuisance alarms or malfunctioning of the algorithms in Video Fire Detection (VFD) systems. Additionally to the problems related to detection, false alarms in VFD affect the retrieval of valuable video-based information about the fire scene used for fire forecasting. Such information includes the smoke layer height and the fire location. By combining VFD with volume sensors a complementary, "multi-sensor" system is created, reducing nuisance alarms and missed detections by the video systems and even decreasing their computational cost. This work starts with a literary review on VFD and nuisance alarms, focusing on nuisance in video detection. This is followed by a description of the volume sensors used, of how the system is created, and of how the respective readings are integrated. For localizing the fire with the volume sensors a 2-dimensional mesh is introduced, whereas for the measurement of the smoke layer height a linear array (of sensors) is implemented. Then, two experiments carried out in a closed, empty car park are described, in which the volume sensor systems were used with different fires and setups. Finally, the results of the experiments are presented and discussed.

Resumen

Una iluminación insuficiente, el vapor y el polvo, entre otros, causan falsas alarmas o mal funcionamiento de los algoritmos en los sistemas de detección de incendios basados en video (VFD). Además de los problemas relacionados con la detección, las falsas alarmas en los sistemas de VFD afectan la adquisición de información valiosa acerca del lugar del incendio, la cual se usa para pronosticar el comportamiento del mismo. Dicha información incluye la altura de la capa de humo y la ubicación del incendio. Mediante la combinación de los sistemas de VFD con sensores de volumen se crea un sistema complementario "multisensor", que reduce las falsas alarmas y las omisiones en la detección por los sistemas de video e incluso disminuye su gasto de recursos computacionales. Este trabajo comienza con una revisión de la literatura sobre los sistemas de VFD y las falsas alarmas. Luego se describen los sensores de volumen usados, cómo se crea el sistema, y cómo se integran las respectivos lecturas de los sensores. Para localizar el fuego con los sensores de volumen se introduce una malla de 2 dimensiones, mientras que para la medición de la altura de la capa de humo se implementa un arreglo lineal (de sensores). Después se describen dos experimentos realizados en un parqueadero vacío, cerrado, en el que se utilizaron los sistemas de sensores de volumen con diferentes incendios y configuraciones. Por último, se presentan los resultados de los experimentos y su discusión.

List of Acronyms and Symbols

2-D	Two-Dimensional
3-D	Three-Dimensional
A_I	First OSID imager (Imager A) for the 2-D Mesh
AMR	Adaptive Mesh Refinement
A_n	OSID Emitter number *n* associated to the first imager (Imager A) for the 2-D Mesh, $1 \leq n \leq 7$
BG	Background
B_I	Second OSID imager (Imager B) for the 2-D Mesh
B_m	OSID Emitter number *m* associated to the second imager (Imager B) for the 2-D Mesh, $1 \leq m \leq 7$
b_m	Constant of the equation of the line formed between imager B and its emitter number *m* in the 2-D Mesh reference coordinate system
b_n	Constant of the equation of the line formed between imager A and its emitter number *n* in the 2-D Mesh reference coordinate system
CCTV	Closed-Circuit Television
CFD	Computational Fluid Dynamics
C_I	OSID imager (Imager C) for the smoke layer depth measurement
C_k	OSID Emitter number *k* in the OSID Array (associated to imager C)
CO	Carbon Monoxide
CO_2	Carbon Dioxide
CP	Total number of crossing points of the 2-D Mesh
CSV	Comma Separated Values
EN	European Standards
FACP	Fire Alarm Control Panel
FDS	Fire Dynamics Simulator by NIST
FG	Foreground
FTDI	Future Technology Devices International
GUI	Graphic User Interface
ID	Identification
IDC	Initiating Device Circuit
IR	Infrared
ISO	International Organization for Standardization
K	Total number of C emitters in the OSID Array
LED	Light-Emitting Diode
LIDAR	Light Detection and Ranging
LWIR	Long-Wave Infrared
M	Total number of B emitters for the 2-D Mesh
m_m	Slope of the line formed between imager B and its emitter number *m* in the 2-D Mesh reference coordinate system

m_n	Slope of the line formed between imager A and its emitter number *n* in the 2-D Mesh reference coordinate system
N	Total number of A emitters for the 2-D Mesh
NC	Normally Closed (Relay)
NFPA	(American) National Fire Protection Association
NIST	(American) National Institute of Standards and Technology
NO	Normally Open (Relay)
OSID	Open-area Smoke Imaging Detection
P_{flames}	Probability of a VFD point corresponding to flames
P_{smoke}	Probability of a VFD point corresponding to smoke
$P_{smoke\text{-}OSID}$	Probability of a VFD point corresponding to smoke based on the detection information from the OSID 2-D Mesh
r_{alarm}	Distance from the 2-D projection of a FireCube point to the closest 2-D Mesh point in alarm
r_{clear}	Distance from the 2-D projection of a FireCube point to the closest 2-D Mesh point without alarm
r_{cp}	Distance between two crossing points in the OSID 2-D Mesh
RSET	Required Safe Egress Time
t_{flames}	FireCube flame probability threshold
TOF	Time-of-Flight
t_{smoke}	FireCube smoke probability threshold
TTL	Transistor-Transistor Logic
UL	Underwriters Laboratories
UPS	Uninterruptible Power Supply
USB	Universal Serial Bus
UV	Ultraviolet
VFD	Video Fire Detection
x_{cross}	x-coordinate of a crossing point in the 2-D Mesh reference coordinate system
y_{cross}	y-coordinate of a crossing point in the 2-D Mesh reference coordinate system
z_{layer}	Smoke layer depth measured from the ceiling with the input of the OSID Array

Disambiguation

Within the following thesis report, some terms can have several meanings or different terms can be used indistinctively sharing the same meaning. It is expected that the context will make clear the meaning of the terms, when it is not explicitly indicated. These terms are:

Crossing point	Refers to the point where three mutually perpendicular planes cross within the VFD 3-dimensional space or to the point where two different lines cross within the volume sensor-based 2-dimensional mesh (the OSID 2-D Mesh).
Detector	The term 'detector' and 'sensor' share the same meaning within all of the text, referring to a physical or virtual device determining the presence of smoke or flames by measuring (or estimating) physical properties in the fire scene.
Frame	Refers to a video frame (the video image at a specific time) or to a serial frame (a structured character chain for serial communication).
Sensor	Refers to a VFD sensor (i.e. a video camera), to a smoke sensor (i.e. photoelectric, ionization) or to a sensor point (defined as a crossing point with detection information within the VFD 3-dimensional space—or FireCube)

Table of Contents

1. Introduction

Detection is a crucial aspect in the event of a fire. It is the first, and triggering, of the events involved in the required time for a safe egress of occupants (RSET) [1]. It also depends on it that the fire service is timely notified about the emergency and that automatic extinguishing systems are activated soon enough [2]. Thus, both for life and property protection, a quick response is very important in the design of fire detection. Traditional fire detectors are based on temperature thresholds, temperature increase rates, radiation by flames, smoke particle interception of gaseous ions, light obscuration by smoke, and light scattering by smoke [2] among others. However, most of these detection techniques (except the flame detection) depend on the transport of smoke or hot gases to the location of the sensor. Such transport delay may be considerably long depending on the situation, especially for large open spaces, and it is desirable to minimize it.

The introduction of video-based fire detection (VFD), in principle, overcomes the transport delay problem as the image analysis can be done immediately, as long as the fire is within the frame, without waiting for gases to reach a specific point. VFD also has the ability to provide information on the progress and spread of the fire and on important variables or states of the premises (e.g. the air entrainment variation due to the breaking of windows or opening/closing of doors) [3]. Several approaches and algorithms have been developed for VFD [3,4,5,6]. However, the best results have been achieved with multi-modal implementations, as compared by Verstockt [3], by integrating the readings from different types of sensors (cameras). Verstockt has also introduced the concept of the FireCube, a multi-view framework based on the images from several cameras to construct a 3-dimensional space where the smoke (and flames) can be detected and traced, providing valuable information for fire spread forecasting.

Both, the multi-modal and multi-view implementations of VFD are to some extent vulnerable to false alarms due to steam, dust, lighting and shadows. False, *nuisance* alarms are not something that traditional types of fire detectors are exempt of. Especially in the case of smoke detectors (usually preferred for a faster response as compared to thermal detectors), nuisance alarms represent a large portion of the total fire alarms [7, 8, 9]. There is a compromise between the immunity to false alarms (related to a lower sensitivity of the sensor) and the promptness of the detection (related to a higher sensitivity) [9] for traditional sensors and such is the case for VFD too. Thus, reducing the sensitivity would sacrifice much of the timely warning that is achieved by this type of detection. On the other hand, combining VFD with traditional detectors can help reducing the false

alarms and even getting additional information from the fire depending on the type of detector.

This chapter briefly describes the multi-modal and multi-view frameworks of VFD [3] and how the latter can be used for fire spread forecasting. It also refers to the false alarm problems experienced by this technology, and to general nuisance alarms caused by traditional detectors, mentioning some implementations of multi-signature detectors intended to reduce such false-positives. Next, different options for combining VFD with other technologies are mentioned, focusing on the implementation of multi-view VFD for large open spaces. Finally the objectives of the work are presented.

1.1 Video Fire Detection—VFD

The increasing use of CCTV (Closed-Circuit Television) for surveillance has resulted in a wide deployment of video cameras in all types of buildings and industries. After exceeding the physically possible amount of cameras to be monitored by the human eye in a lot of installations, the implementation of *video analytics* (automatic video image processing and decision algorithms) seems necessary. As a matter of fact, there is currently a broad use of video analytics in applications including traffic control, perimeter security, and facial recognition [4], among others.

The concept of video analytics has been extended to fire detection by the development of algorithms to detect smoke and flames. By using the video input of analog or digital cameras, these algorithms use different techniques to identify flames and/or smoke based on changes of properties including brightness, contrast, edge content, motion, dynamic frequencies, and pattern and color matching [6]. Different types of systems have been designed, some with the input of the camera(s) being processed in a central unit and others where the processing is done at the camera itself. Depending on the target of the algorithm (i.e. detect flames, detect smoke, or both) the type of camera brings different capabilities and limitations. By integrating the capabilities of the different types of cameras, a multi-modal framework can be implemented, enhancing the performance of VFD. Also, by incorporating the images of different cameras (of the same or different type) from the same scene, a multi-view framework can extract additional information from the fire, like its location, direction, and dimensions [3].

1.1.1 *Multi-Modal VFD*

Infrared (IR) illuminators and IR sensitive cameras are used to compensate for low light conditions in the scenes [6]. The information from IR cameras is also compared to the information from visual cameras (cameras that work within the visible spectral range) in most multi-modal video analyses to filter objects with appearance or behavior similar to that of smoke or flames; those that can be seen in the visual images and behave like smoke and cannot be seen in the IR images are considered candidate smoke regions [3]. The spectral ranges in which IR cameras operate are the short, medium, and long-wave infrared ranges, being the former the one closer to the visible bands and the latter, LWIR (8-12 μm), the one with less visual perceptibility and higher thermal perceptibility. Cameras with this type of spectral range focus mainly on the temperature of objects, being a desirable complement to visual cameras in a multi-modal framework.

Verstockt [3] also introduced the research on multi-modal VFD with time-of-flight (TOF) cameras. These types of cameras use frequency modulated IR signals to illuminate the scene and analyze the signals reflected by every pixel (of the objects in the scene) providing information of the depth, or distance to the camera, and amplitude, or strength of the reflected signal. TOF cameras, best used for indoors purposes due to the distance limitations (<10m), are integrated to visual cameras by Verstockt to create a multi-modal visual-TOF flame detector, with satisfactory results (minimum false alarms and flame detection of ≥ 89%). Multi-modal VFD provides an additional way of fire detection, experimentally proven to surpass the performance of some traditional detectors, especially for outdoors implementations. Moreover, additional information can be extracted from a scene under a multi-view framework, allowing the identification of the origin, size, and location of the fire, among others. As it will further be discussed, this thesis introduces the combination of volume sensors with existing VFD frameworks, which can also be perceived as a multi-modal approach (or rather “multi-sensor” in which volume sensors and video sensors make a combined sensor).

1.1.2 *Multi-View VFD*

Several cameras that monitor the same scene from different viewpoints can be used together, rather than separate simple fire detectors that indicate if there is a fire or not. When used together, the fire detection information from each of them can be overlapped improving the reliability by creating redundancies. This information can also be mapped in several horizontal and vertical planes, generating a 3-dimensional space with the information from the crossing points of these planes. Such approach is the one introduced by Verstockt’s FireCube [3]. In this multi-view framework, the

cameras detect the fire separately, and then the detection information from the different cameras is projected in horizontal and vertical planes slicing the scene. The overlapping results at each plane are averaged and the crossings of all of the planes are extracted to create the 3-dimensional grid, or FireCube. The FireCube acts like a space of virtual sensors, based on the information processed from the different cameras monitoring the scene simultaneously. This grid of sensors provides information about the location of the smoke, its growing and size, and its direction of propagation. Two cameras are enough to build a grid, however a third one is often used for a higher accuracy of the detection in the grid. Fig. 1 shows an example of the smoke localization using the mentioned framework.

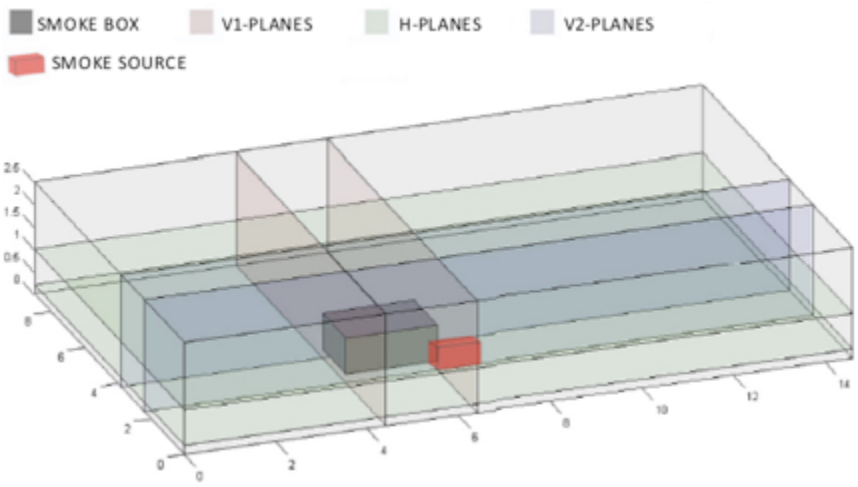

Figure 1: Smoke localization with multi-view framework (Taken from [3], modified)

The smoke is represented by a box that is updated every frame. The example shows four vertical planes, two in each direction (i.e. two V1-planes and two V2-planes), and two horizontal planes, bounding the smoke box. Based on the smoke boxes at each frame, the multi view framework can generate spatio-temporal characteristics of the smoke, which can be processed to determine the growth and propagation. It is this processed information what works as an input to the forecast, or prediction of the evolution of the fire.

1.1.3 *Fire Forecasting with Multi-View VFD*

Fire forecasting is a recent approach [3, 10] in which the fire development is predicted by performing calculations based on fire models using observations of physical quantities from the fire scenario as inputs. Because of the importance of a short time in the calculations, i.e. shorter than the real time of the fire, models based on Computational Fluid Dynamics (CFD) result too resource and time

consuming and are not currently used in fire forecasting. Alternatively, simpler numerical models, like zone models (e.g. Zukoski's two-zone model in [10]), are preferred to produce forecasts for their lower time consumption, or small 'lead' time.

Fire forecasts aim to provide the fire service with useful predictions about the size of the fire (smoke and flames) and its spread. By means of the use of sensors, the values of physical quantities like temperatures, pressures, and velocities, among others, are measured and used by the forecast algorithm to accelerate or correct the predictions previously done by the models, like a feedback process being continuously updated. Fig. 2 shows a representation of this process.

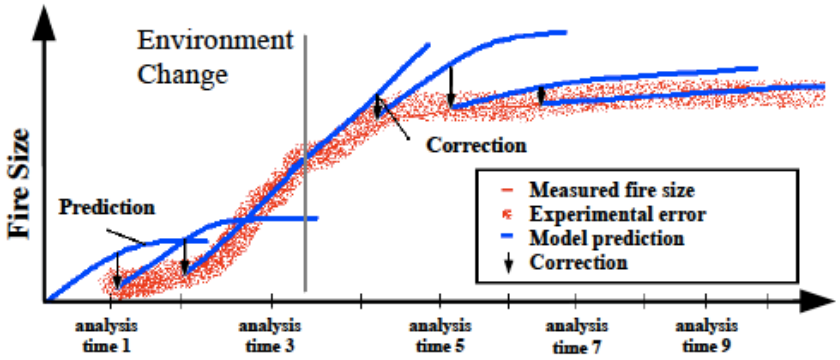

Figure 2: Representation of model predictions and sensor-driven corrections in fire forecasting
(Taken from [10])

Under the multi-view VFD framework proposed by Verstockt [3], the capability of providing information about the size, growth and propagation of the smoke is used together with the outcome of two-zone models for fire forecasting. On the other hand, a multi-modal VFD system could also provide useful information about the scene of the fire, like temperatures measured with thermal (IR) cameras, or flame and smoke dimensions from visual cameras.

1.1.4 *False Alarms with VFD*

As any of the other technologies for fire detection, VFD is not immune to false alarms. Actually, video sensors present illumination-related false alarms and missed detections (especially visual video sensors). Most basic detection algorithms are based on visual images, as in the case of color detection and moving object detection. While the former focuses on the color of the pixels and compares it to the ranges of color of smoke and flames, the latter makes use of movement detection algorithms on the frame to subtract stationary non-smoke objects. However, both

depend on the illumination (and quality) of the scene on the frame, and variability in color, lighting, density, background, and reflections (especially of flames) make them vulnerable to false alarms. Types of false/nuisance alarm sources with VFD in industry include heat and light sources, arc welding, torch cutting, sparks from grinding metal, movement of machinery and lens contamination [6]. Two examples of frames that have led to missed detections can be seen in Fig. 3.

More sophisticated algorithms for detection have been implemented; these include energy analysis, spatial difference analysis, dynamic texture and pattern analysis, and disorder analysis [3], where the detection is based on temporal analyses and property variations. However, the more complex the detection algorithm gets, the more time consuming the detection becomes. A slower VFD detection is not something desirable as an important requirement for detection systems is a fast response. This has been a reason for the introduction of multi-modal systems, where other types of cameras than visual (e.g. LWIR, TOF) are used, as mentioned in Section 1.1.1, to avoid the disadvantages of visual ones. The better performance of these systems, compared with single visual VFD systems has been experimentally proved, however they are still vulnerable to steam and dust false alarms.

Figure 3: Examples of VFD false negative frames (Taken from [3])

1.2 Nuisance Alarms and Redundancy

The credibility of detection systems is reduced when the end, sensing, devices provide a large number of nuisance alarms [5]. Actually, the problem of false alarms caused by sensor malfunction or misplacement is the leading cause of firefighter responses to false alarms in the United States. According to NFPA statistics [7] in 2009 fire departments went to 16 false alarms for every 10 fires and 45 false alarms for every 10 structure fires. This means that false alarms make more than half of the total fire alarms that reach the fire departments. And out of these false alarms, NFPA reports that a 32% of them were caused by system malfunctions and 45% were

caused by unintentional activation of the systems. Reducing nuisance alarms due to system malfunction might be controlled by a proper maintenance of the systems. Nevertheless, the larger and more complex systems become, the greater odds that single components (sensors) can fail. The unintentional activation is related to both the misplacement of sensors and the incorrect selection of the sensor types, which can in principle be controlled or corrected. However, this type of activation is also related to other uncontrollable causes (e.g. environmental causes) that result in false fire detections. Whichever the cause or origin of the false alarm, a large amount of false alarms presented in a system results in a system in which neither the public nor the fire department believes.

The reduction of sensor sensitivity is a method for increasing immunity to nuisance alarms [14]. This results, however, in longer response times, something that cannot usually be accepted. For the case of photoelectric smoke detectors, which are most traditionally used for their fast response [11], there has been research to improve or replace simple algorithms based on thresholds with more complex algorithms based on fire (smoke) signatures [12]. However, there has been more research and a significant use in real installations of multi-signature detectors [13, 14, 15]. Thermal, ionization and photoelectric smoke detectors, and CO detectors have been combined using neural networks trained with models of fire growth and smoke spread, proving to be a good approach for early detection with reduced nuisance alarms or misdetections [11]. Cargo compartments in aircrafts have also been a subject of research for the development of fast, reliable fire detectors based on the combined detection of smoke and measurement of combustion products like CO and CO_2. The combination of these measurements has resulted in faster detection with less nuisance alarms as well.

As it has been proved for smoke detectors, a redundancy or complement with other types of sensors results in the improvement of their performance and response. It would be expected, also, that the nuisance alarms and misreading related to the VFD technology decreased by combining the cameras with other types of sensors. Additionally, the information from the VFD systems can help with the verification of the alarms raised by the other sensors.

1.3 Combining VFD with Other Technologies

VFD experiences nuisance alarms due to illumination, steam and dust. Just as smoke detectors, also prone to false alarms, have been combined to other types of detectors to develop more effective detectors or systems, VFD can be combined to other types of sensors to verify and reduce the false alarms. Firstly, using sensors that don’t depend on illumination and/or are immune to steam/dust would help the

detection problem directly. It would also be desirable that the sensors had a better (more efficient) power supply reliability, given that for VFD systems the 24-hour standby power operation, usually required by alarm systems, implies complex (expensive) backup solutions like a mains UPS for the central unit and battery backed supplies for the cameras (as a minimum) [5]. Also, due to the illumination-dependence of most (visual) VFD systems, the combination with sensors that don't depend on illumination helps overcome the limitations on the minimum lighting levels required, also related to the power supply reliability (of the lights). The combined system can also benefit from the readings of the VFD, verifying detections of the other sensors with the video detection data.

Additionally to the benefits against nuisance alarms of combining VFD with other sensors, these inputs can also help reducing the resource consumption (processing times) of the 3-D algorithm of the multi-view framework (Section 1.1.2). The FireCube is calculated every frame, which together with a more accurate localization (i.e. larger amount of slicing planes) results in an increasing computational cost [3]. An external input that could help determine the parts of the frame that need to be updated or recalculated would result in a decrease in the computational cost or would allow the increasing of slicing planes of the 'relevant' section of the fire scene, thus increasing the accuracy of the localization.

Several types of sensors could be considered for the combination with VFD. Point detectors, for instance could be useful in small, closed areas. However, for these types of areas the benefit of VFD over other sensors is not much. It is of a greater significance for this project, then, the combination of VFD with other sensors for the detection and forecast of fire in large, open spaces. The sensors considered are thermopile arrays, Light Detection and Ranging (LIDAR) sensors, and Open-Area Smoke Imaging Detection (OSID).

1.3.1 *Thermopile Arrays and LIDAR*

Thermopile arrays are electronic devices constructed with thermoelectric materials (materials that generate a voltage proportional to the temperature difference applied to two junctions of two of such materials), which capture (IR) radiation thus being able to measure the temperature of objects [16]. These sensors have been recently used for burglary alarms (intrusion detection) and have also been applied in space science applications [16, 17]. With 2-dimension (2-D) thermopile arrays, it is possible to have a thermal representation of a scene, as shown in Fig. 4. Under a multi-view visual framework, a verification based on thermal information would help reduce false alarms linked to the visual cameras. However, the benefits are similar to the ones by combining the visual cameras in a visual-IR multi-modal framework.

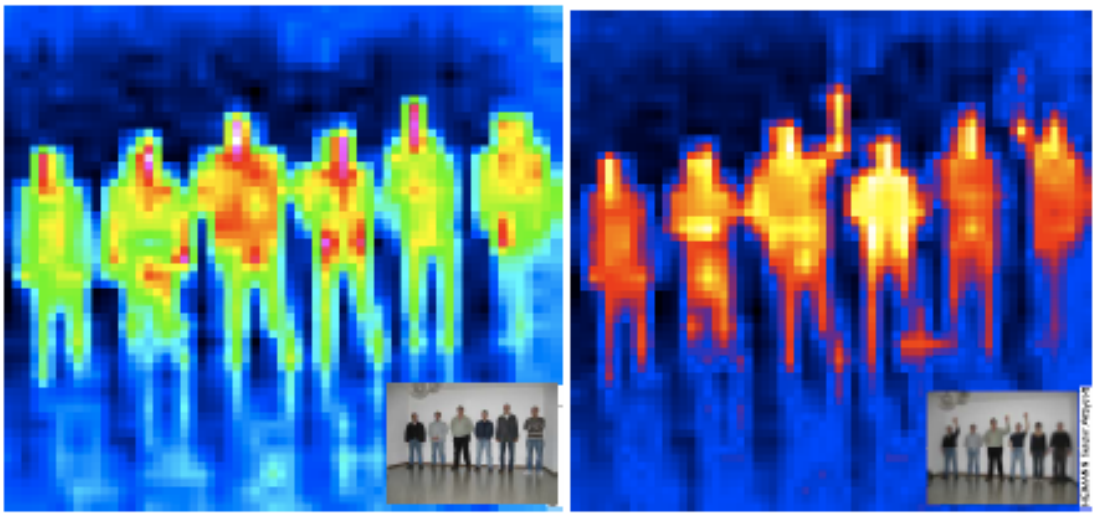

Figure 4: Thermal image showing person detection (Taken from [16])

LIDAR, on the other hand, is an imaging technology based on laser light. By illuminating the target and analyzing the backscattered light, LIDAR sensors can measure distance to the target and properties like (gas) densities, temperature, pressure, wind, humidity, and concentration [18]. With such capabilities, it is possible to obtain 3-D images when combining LIDAR information with visual images [19, 20] and get additional information on materials properties. LIDAR is widely used in outdoors applications, for geology, meteorology, astronomy and military purposes, making it adequate for the combination with VFD in outdoor spaces, initially. The main benefit being the illumination-independence of these types of sensors (as they work with their own laser light source) and the additional information on the gas properties, which would improve the decision on candidate smoke regions. However, as the current research and applications of this technology have been done in outdoor spaces, it is not suitable for this project. A height-encoded LIDAR image of an urban scene is shown in Fig. 5.

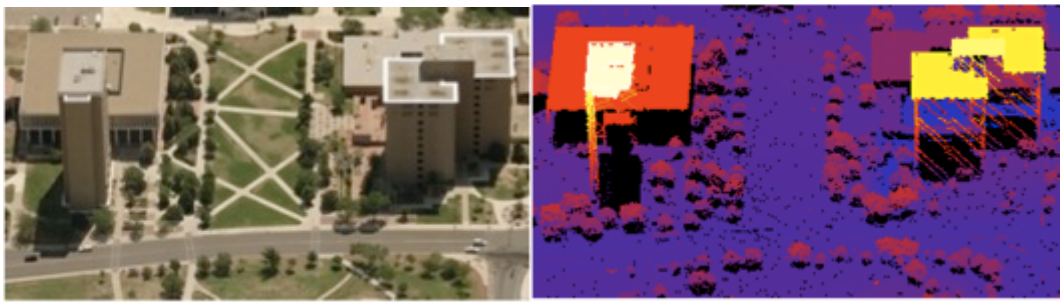

Figure 5: Height-encoded LIDAR image of an urban scene (Taken from [20])

1.3.2 *OSID*

Open-Area Smoke Imaging Detection, OSID, is a detection technology developed by Xtralis in which the concept of the traditional beam detector is enhanced. As seen in Fig. 6, traditional beam detectors transmit one IR light beam (by e.g. an IR Light-Emitting Diode—LED), which is received by a photosensitive device, usually a photodiode, and smoke is detected by comparing any attenuation or scattering of the light with predefined sensitivity thresholds [21].

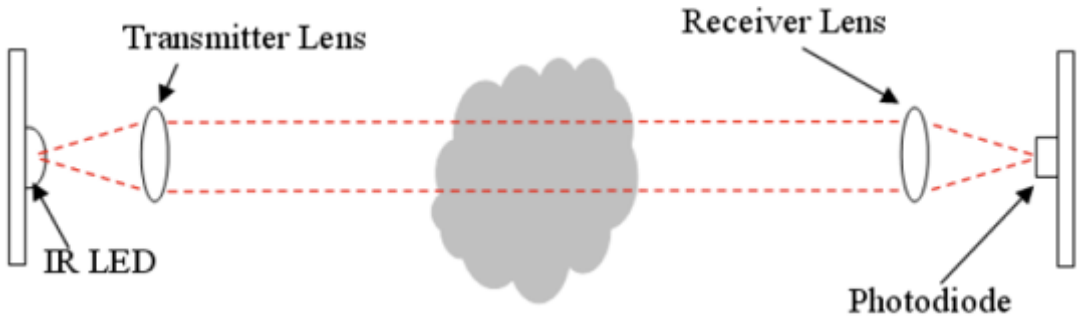

Figure 6: Traditional beam detector operation (Taken from [16])

OSID, on the other hand, uses wide-angled beams containing sequences of ultraviolet (UV) and IR light pulses, sent from an emitter with a unique coding, which are captured by an imager that compares between the two types of light. OSID emitters project conical beams of about 10° width and imagers locate and detect these signals by means of a video imaging chip. Imagers are also fitted with CCTV type lenses that can vary from 10°, 45°, and 90° field of view, allowing the association of up to 7 emitters with a single imager and covering wide areas or volumes. A simplified representation of the operation of a single-emitter implementation of OSID is shown in Fig. 7. Traditional beam detectors are prone to generating false alarms due to object intrusion (e.g. banners, balloons, insects, birds) or dust within the path of the beam. These objects can cause the predefined light attenuation (or light scattering threshold) with a considerable probability, depending on the installation conditions, thus triggering nuisance alarms. For OSID it is possible to discriminate between these false positives and real smoke alarms, as the dust or intruding objects have bigger particles affecting both, the larger wavelength IR light and the shorter wavelength UV light, while the smaller particles of real smoke affect the UV light predominantly [22]. By software, OSID examines the strength and behavior of both signals and determines if the conditions are such that an alarm needs to be raised.

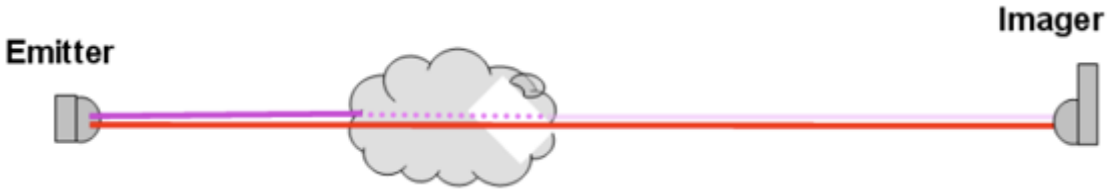

Figure 7: Linear OSID operation—simplified (Taken from [16])

OSID has been tested with UL and EN tests fires as well as with nuisance sources including the ISO standard dusts, steam, and talcum powder showing a consistent responsiveness to all of the common smoke types, as reported by Xtralis [21]. This performance against nuisance alarms makes OSID a good type of detector to combine with VFD in order to overcome the false positives experienced by this technology especially under difficult lighting conditions, or in the presence of shadows, smoke or dust. Also, the possibility of covering wide areas (or volumes) with multiple emitters associated to a single imager makes OSID a suitable technology for the intended large, open spaces for the VFD system.

1.3.3 *Combination of VFD with OSID*

Due to the benefits mentioned, and the possibility to make experiments with OSID detectors supplied by Xtralis, these were the ones used for the design of an algorithm to integrate their information with the information on the multi-view VFD framework. A representation of the proposed combination and the algorithms interactions can be seen in Fig. 8. As it can be seen, the two systems interact supplying detection information to the other so that both verify their fire alarms.

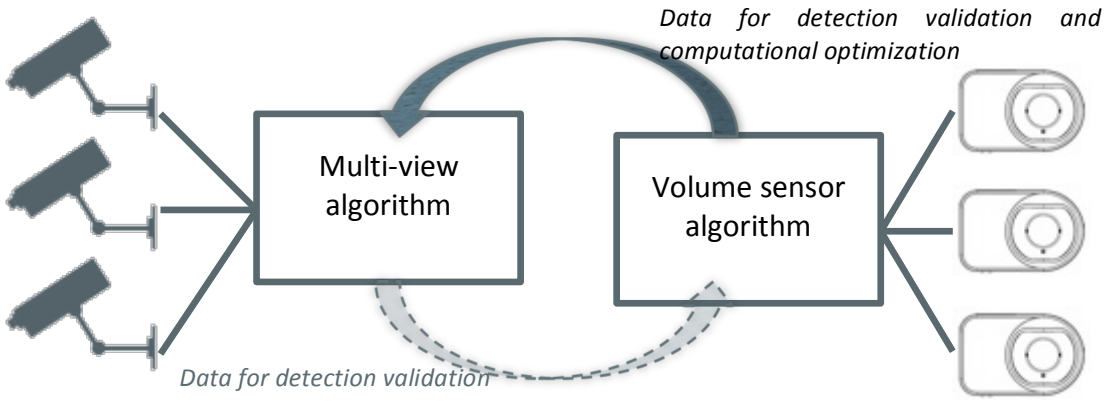

Figure 8: Combination of VFD with OSID

OSID detectors can be installed in several configurations, covering lines, areas and even volumes. Depending on the configuration of these detectors, the algorithm proposed would be able to validate a smoke alarm, validate the location of the smoke and/or supply information for the fire forecast (e.g. the depth of the smoke layer).

1.4 Objectives

OSID detectors will be combined with VFD for smoke alarm verification, smoke localization validation and smoke layer depth measurement. The main purpose of this work, rather than verifying the nuisance alarm immunity of OSID, is creating an algorithm for integrating the output from OSID with the information from VFD. As mentioned in Section 1.3.2, Xtralis has performed experiments with OSID with nuisance sources including dust and steam, with satisfactory results. However, the results of the experiments are proprietary and have not been published to date. Thus, a better immunity to dust and steam of OSID compared to VFD is taken as a true hypothesis for this work. Fig. 8 shows the proposed, complete, combination of VFD with OSID, with the two systems sharing information (i.e. giving feedback) to each other. The initial approach in this project, however, focuses on the processed information from the OSID detectors and its integration with the VFD detection measurements within the multi-view framework (the feedback from the VFD system to verify detections in the OSID represented by the dashed arrow outside the scope of the thesis). The specific objectives of the work are then:

- To design an OSID-based system to detect and locate smoke and to measure the smoke layer depth.
- To design the integration of the processed information from OSID detectors with the VFD detection information within the 3-D space of the FireCube.
- To implement and test the OSID-based systems with in real scale and with real fire.

2. Methodology

For the combination of VFD with OSID it is important that the information from either system is compatible with the other, so that the data interaction described in Section 1.3.3 is possible. As seen in Fig. 8 from the same section, the data received by the OSID algorithm is to be used for detection validation whereas the one received by the multi-view algorithm is used both for detection validation and computational optimization. In both cases, the spatial representation of the scene or covered area should match between both algorithms so that the location of detection points can be transmitted and correctly interpreted. This chapter explains how the readings from independent OSID emitters are captured and integrated by software to generate the data that is sent to the multi-view algorithm. It also mentions how the information from the multiple cameras is handled within the multi-view framework.

The nuisance alarm reduction by the combination of VFD with OSID is mainly aimed for a better performance of first, smoke detection and localization and second, smoke layer depth measurement as an input for video-driven fire forecasting. Further sections of this chapter explain how the OSID detectors are set up for both purposes, what the algorithms are to generate the mentioned data, and how the combination of both systems is carried out within the VFD multi-view framework by using the information received from the OSID detectors. The last part of this chapter is dedicated to the description of the experimental set-ups made for testing the smoke detection/localization and the determination of the smoke layer depth with OSID and VFD systems on the same scene.

2.1 OSID Data Handling

The output signals from any OSID configuration are always generated by the imagers. These have NO/NC relay outputs for Initiating Device Circuits (IDCs) connected to Fire Alarm Control Panels (FACPs), which indicate whether there is a fire alarm or not. They also have LEDs for visual indication of the state, providing additional information like the ID of the emitter under alarm (for multiple-emitter configurations); the LEDs blink with codified pulses to represent the different emitters [22]. An output signal meant to be used with a remote LED drives the same pulses. Additionally, the imagers can be monitored through a USB cable connected to a computer with a monitoring/diagnostic software application. A representation of the circuit (‘termination’) card of the imagers can be seen in Fig. 9; the IDC output, the LED output and the USB-cable output are indicated.

There are different ways to retrieve the information from the imagers to process it and transfer it to the VFD algorithm and this section explains two of them: an offline option by using the logged data from the Xtralis - OSID Diagnostic Tool and a real-time option by reading the pulses from the remote LED output in the termination card of the emitter. For the computer algorithm presented in this project, and the experiment set-ups discussed in Section 2.5, the way of retrieving the data from the ODIS is the offline option.

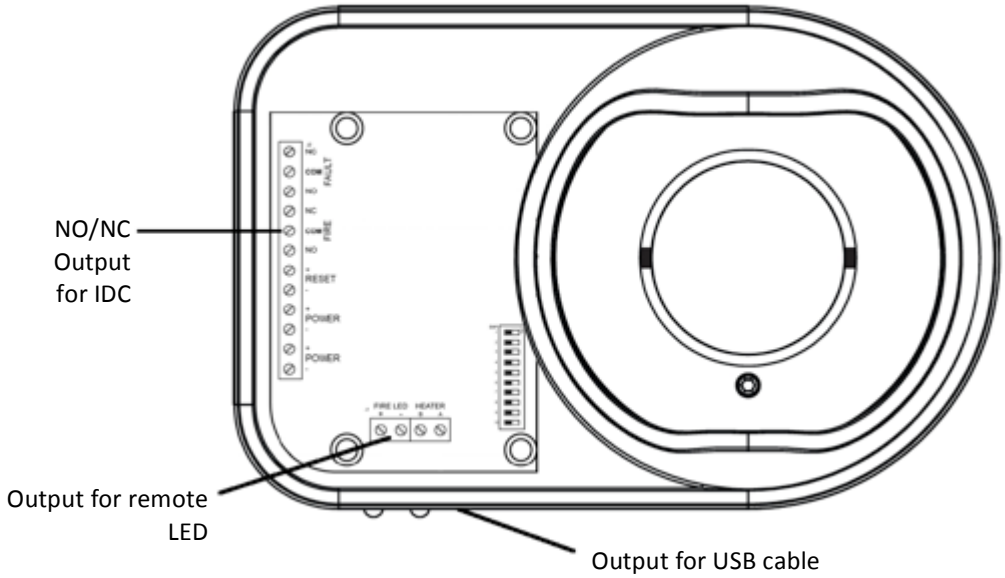

Figure 9: OSID imager outputs—termination card (Taken from [22]—modified)

2.1.1 Offline Data

OSID detectors are originally designed to work together with a FACP rather than alone. For this reason, the main outputs are the relays for the IDC. However, for installation, calibration, or diagnose purposes, an FTDI[1] cable can also be connected to the imager and used together with the Xtralis – OSID Diagnostic Tool, with its Graphic User Interface (GUI) shown in Fig. 10. The software tool allows checking the live attenuation of the UV and IR signals from all of the emitters associated to an imager as well as observing a live view of the frame viewed by its video imaging chip. Additionally, the alarm or trouble estates of each of the emitters can be monitored, with a description of the type of trouble in case there is any. The attenuation of the UV and IR signals of all the emitters is sampled three times every second and this data, as well as any event from any emitter or the imager, are logged. The event log

[1] FTDI (Future Technology Devices International) cables drive data from a serial transmission (at the imager in this case) to a USB plug to be connected to a computer.

files are CSV (Comma Separated Values) files with open access. However, the attenuation sampled data log files are codified and currently only accessible by Xtralis. For the work done in this thesis, the codified files were converted to CSV files by Xtralis and all of the handling of offline data is based on the availability of such files. The sampled data log files contain rows with the exact date and time of the sampling, the ID of the respective emitter, the percent attenuation of UV and IR beams of the emitter, and the alarm estate. The OSID detectors can be configured to have a high, medium, or low sensitivity, and based on this, and the comparison between the UV and IR signal levels (see Section 1.3.2), a fire alarm is triggered and the alarm estate is varied in the log file. As it will be further described, for the experiments designed for this thesis a high sensitivity was used; the lower ones are generally used in environments without a clear air. With the CSV sampled data log files, the estate of all of the emitters is verified by checking on the alarm and then processed either for detection and localization, as discussed in Section 2.3.2, or for the smoke layer depth measurement, as discussed in Section 2.4.2.

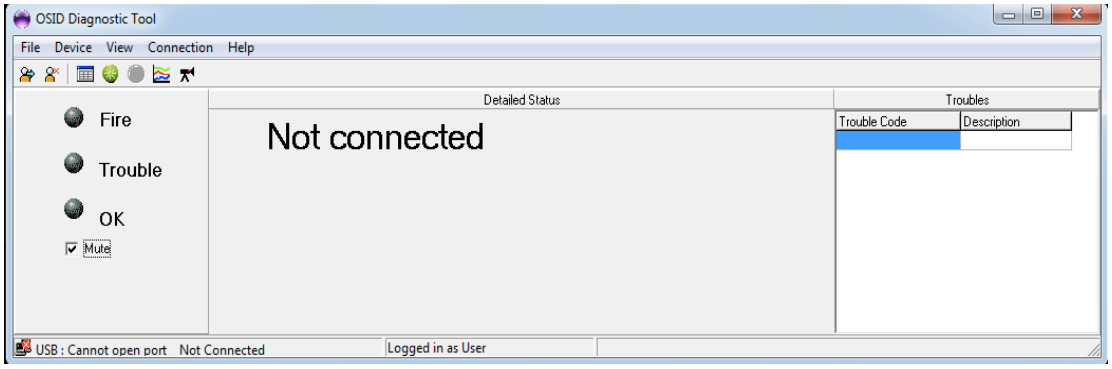

Figure 10: Xtralis – OSID Diagnostic Tool GUI

2.1.2 Real-time Data

The processing required either for the detection and localization or for the smoke layer depth measurement with the OSID detectors is minimum, as will be seen in Section 2.3.2 and 2.4.2. Thus, it is possible to think of a real-time processing of the alarm estate of the emitters. The simplest way to obtain the real-time estate of the emitters would be through the FTDI cable from the imager. However, the serial data received by the computer through this cable is also codified and proprietary. Without access to this output from the imager, another option is to use the remote LED output shown in Fig. 9. The codes used by the signals on the remote LED output of the imager can be seen in Fig. 11 for the cases of all emitters in alarm, one emitter number ‘n’ in alarm, and emitters 2 and 3 in alarm, respectively.

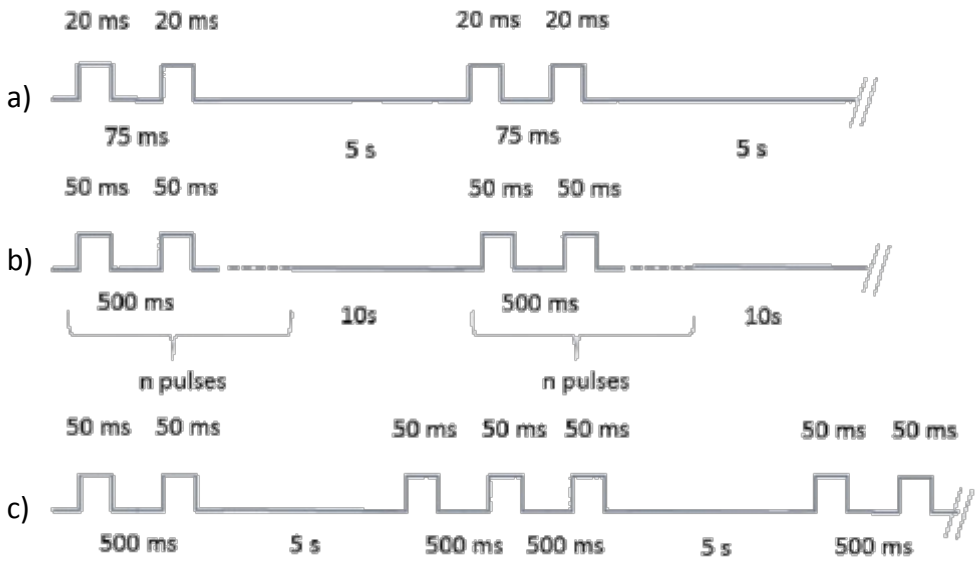

Figure 11: Remote alarm LED codes (Provided by Xtralis) for a) All emitters in alarm, b) Emitter 'n' in alarm, and c) Emitters 2 and 3 in alarm.

As it can be seen in the figure, 20ms pulses indicate that all the emitters are in alarm while 50ms pulses are generated when only one or some are in alarm. This output is meant to be connected to an LED rather than to a computer so the use of an electronic interface is necessary. The block diagram of the proposed OSID-USB interface is shown in Fig. 12.

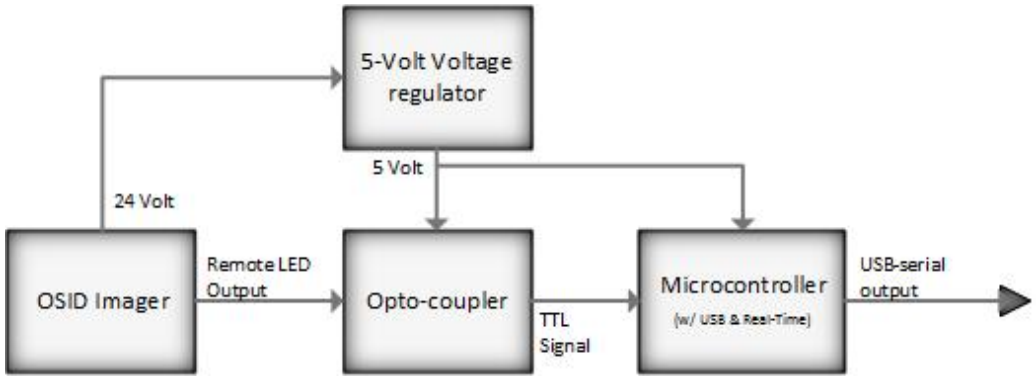

Figure 12: Proposed OSID-USB interface—Block diagram

With the main components being a voltage regulator, an opto-coupler and a microcontroller the aim is to supply, through USB serial communications, a frame containing the alarm status every second similar to the data from the sampled data log file discussed in Section 2.1.1 (without the UV and IR attenuation information). The voltage regulator and the opto-coupler are used to translate the current-driven LED output from the OSID imager into a TTL voltage level suitable for the microcontroller.

The latter is in charge of determining if there is an alarm and from which emitter it is, of recording the time at which this alarm was received, and of preparing the serial frame to be sent to the computer through USB. Thus, the microcontroller used should have USB host capability and a real-time clock and calendar. For determining if there is an alarm and its precedence, the microcontroller monitors the voltage-translated signal coming from the remote alarm LED output of the imager and runs an algorithm like the one represented by the flowchart in Fig. 13. The microcontroller waits for a change in the input signal and, after receiving one, it checks if the step is a growing or a decreasing one. Based on the structure of the code as shown in Fig. 11, the microcontroller concludes if all the emitters are in alarm or it determines which of them are, saving all of the consecutive alarms. With the previous information, and recording the exact time and date of the alarm, the microcontroller prepares the serial frame and sends it to a USB cable connected to the computer. With this, the same information that is used from the CSV sampled data log files discussed in Section 2.1.1 becomes available in real-time.

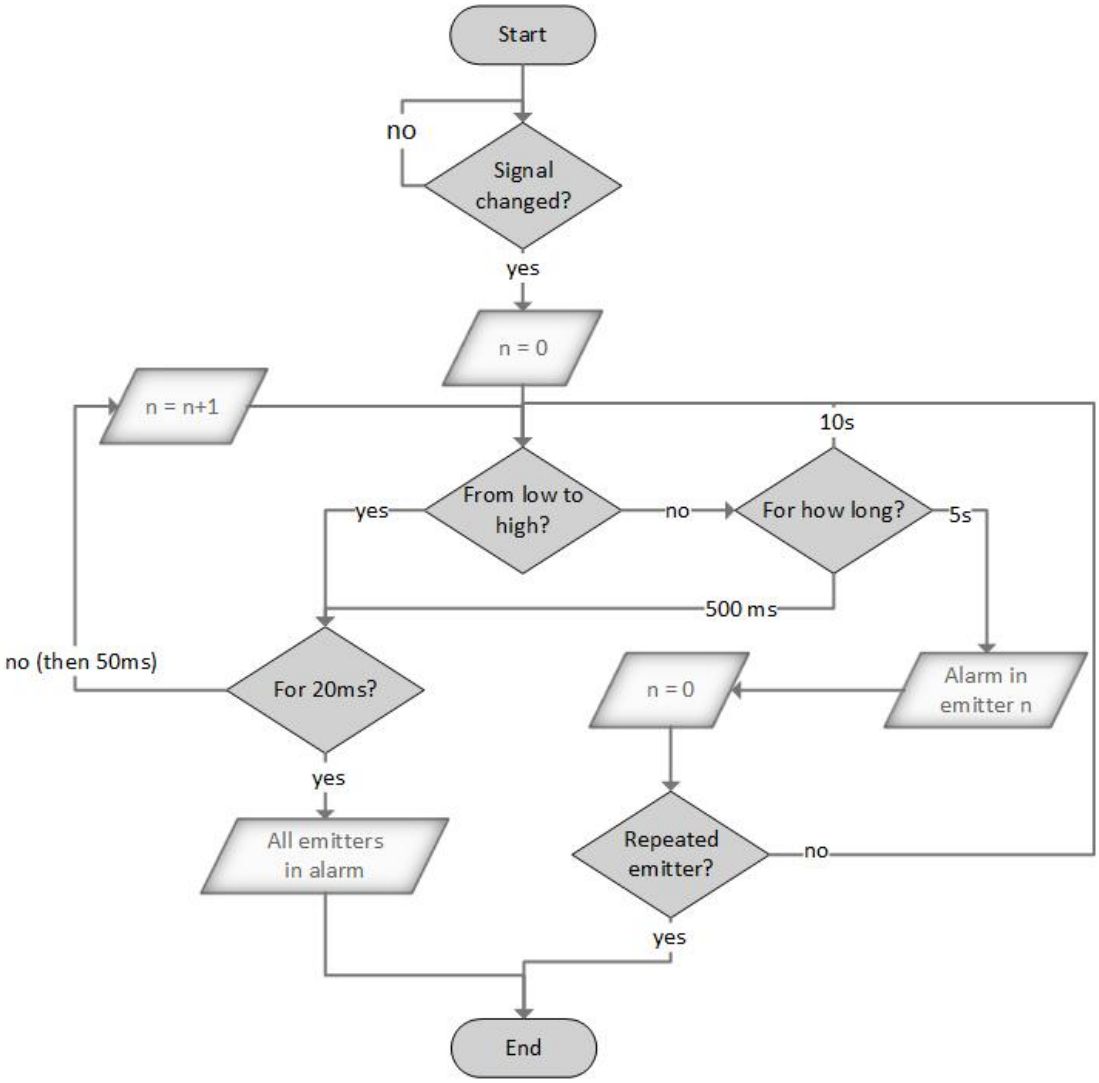

Figure 13: Microcontroller alarm identification algorithm

2.2 VFD Data Handling

The flames/smoke detection information from several cameras is united to create the FireCube as mentioned in Section 1.1.2. To create the 3-D space starting from single-view 2-D images the VFD algorithm uses geometry (i.e. homography) to project the 'useful' information onto a reference, 3-D, coordinate system [3, 23]. The non-useful information corresponds to the elements on the frame that do not change their position/location (i.e. do not move) and are known as the background (BG). The information of these elements is not projected to the 3-D space and is not taken into account for the rest of the VFD algorithm. On the other hand, the information of the moving objects, or foreground (FG), is projected from the different camera views on different planes on the reference coordinate system. These planes are uniformly distributed on the three directions: parallel to the front, parallel to the sides, and parallel to the bottom. The projected information is the outcome of any of the possible VFD techniques mentioned in Section 1.1 and corresponds to the probability of the (moving) point being flames or smoke—P_{flames} and P_{smoke} respectively. At every crossing of horizontal plane with two perpendicular vertical planes a point is extracted with the set of all of these points forming the FireCube. The resulting type of each point in the FireCube (i.e. BG point or FG point after a second BG/FG analysis) depends on the average of the probabilities from the same point at each of the intersecting planes. This second BG/FG analysis (also called grid analysis) is done by comparing the average of P_{flames} and P_{smoke} at each point to respective thresholds t_{flames} and t_{smoke}. In case the average of P_{flames} or P_{smoke} exceeds the threshold value, the point is considered a FG point. As done in [23], this can be written in the form

$$\text{FireCube}[x', y', z'] \rightarrow \begin{cases} FG, & \text{if } \overline{P_{flames}[x', y', z']} \geq t_{flames} \\ & \text{or } \overline{P_{smoke}[x', y', z']} \geq t_{smoke} \\ BG, & \text{otherwise} \end{cases} \quad (1)$$

where x', y', and z' correspond to the coordinates of the reference coordinate system. The result is a three-dimensional grid of points in which the fire detection information from single-view images is averaged. Then, each of the points of the FireCube acts like a flame/smoke sensor more 'robust' than single-view VFD systems. The resulting 'sensor' points of the crossing of the planes in a FireCube can be seen in Fig 14. In the graph, the detected points are on the front vertical plane. After the grid analysis, the FireCube is also cleaned-up by using spatial and temporal filters [3, 23]. The spatial filtering is carried out by using weighted median filters, which are applied to every point in the grid and take into account the values of surrounding points to calculate the statistical median of the set. By using this value, the spatial filtering solves noise problems in the FireCube. The temporal filtering is used for removing temporal misdetections.

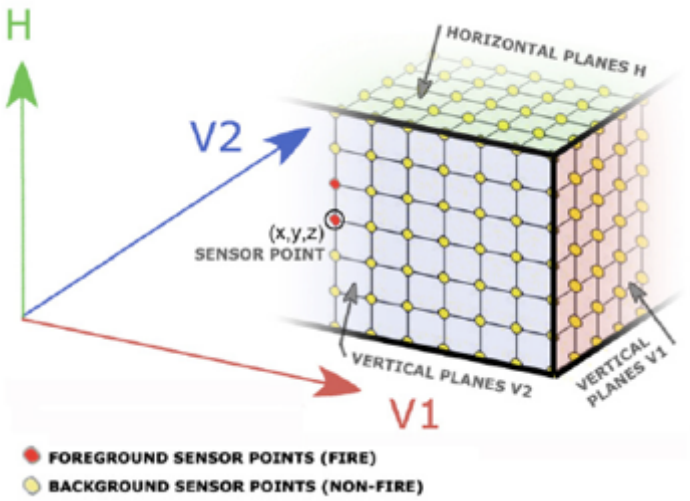

Figure 14: FireCube—Grid accumulation of horizontal and vertical planes (Taken from [23])

With the filtered FireCube, a 3-D space in which a set (or sets) of points representing the flame/smoke regions is obtained. The VFD localization framework, based on the FireCube, further splits this region into two different subregions or bounding boxes: one for the buoyant fire plume and one for the smoke layer. This is done by means of an adaptive bounding box algorithm in which the smoke layer box is first created by iteratively reducing the vertical dimension of the whole region in the upside direction until the 10% or less of the resulting box is filled with BG points. The remaining FG points are merged into another box to create the fire plume box. Fig. 15 shows an example of a FireCube with the two bounding boxes generated. These two bounding boxes can be used within the FireCube to locate the fire, as well as to analyze its evolution and extract important plume characteristics like its size (radius) and time variation; also the smoke layer height and smoke filling time can be extracted from such an approach.

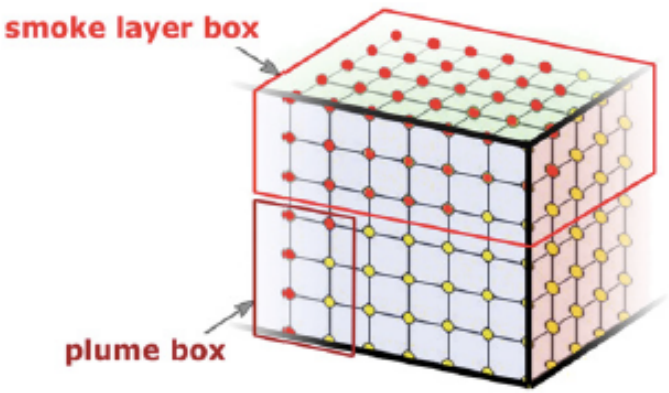

Figure 15: FireCube—Adaptive bounding box strategy for splitting the fire region into plume and smoke layer box (Taken from [23])

2.3 Smoke Detection and Localization

Fast fire detection can help reduce or avoid great damage to people and properties. The time advantage of implementing VFD fire detection has been discussed in Chapter 1, compared to other types of sensors that have a transport delay (of the fire gases getting to their location) associated. In Section 1.1.4 it has been further discussed about the nuisance alarm/misdetection problems linked to VFD systems. For improving the nuisance alarm performance of VFD, specifically of the multi-view VFD framework of the FireCube, it is proposed in Section 1.3.3 the combination of VFD with OSID detectors. The first approach of such a combination is the detection and localization of smoke within a specific area covered by both, the VFD cameras and the OSID detectors.

As mentioned in Section 2.2, the detection results coming from the single-view VFD algorithms in the multi-view framework are in the form of probability values of the specific point corresponding to flames (P_{flames}) or smoke (P_{smoke}). There are different approaches, or techniques as discussed in Section 1.1, to detect smoke or flames in the frames captured by video sensors and any of them could be used with the multi-view approach of the FireCube. The main techniques of the flame detection algorithm used for the FireCube by Verstockt [3, 23] are: Dynamic Background Subtraction, in which the video frames with nothing but BG objects (i.e. everything in the image is still) are removed; Flame Color Rate, in which the objects with the least resemblance to flames are eliminated based on their color and how close it is to the red-yellow range; and Principal Orientation and Bounding Box Disorder, in which the dynamic properties of flames (in terms of the degree of disorder of their time variation) are used to differentiate them from simple hot objects (e.g. that could be moving/moved and have a red-yellow color). The smoke detection algorithm also subtracts the non-moving video frames initially and analyzes the frames by: Boundary-Area Disorder, in which the degree of disorder of the variation of the perimeter and area of objects in the video framed is analyzed and its 'roughness' is calculated to determine how similar the objects are to smoke; Energy Disorder, in which the energy value variation of objects is analyzed over time; and Chrominance Disorder, in which the change in time of chrominance of the regions is analyzed. After applying all of the previous flame and smoke detection techniques, each of them results in a probability number which is then averaged respectively to obtain the value of P_{flames} or P_{smoke}.

On the other hand, the detection in the OSID detectors is done by comparing the attenuation of the UV and IR signals sent from the emitter(s) to the imager. The decision parameters and details of the comparison between the signals are confidential from Xtralis. However, it is known that the basic difference between the UV and IR signals is that smoke will have smaller particles than other elements that

might block the beam between the emitter an imager, thus affecting the shorter wavelength UV signal predominantly. So, OSID detectors basically wait for any kind of medium interfering the signal between the emitter and the imager and then, by comparing between the UV and IR signal attenuation, decide if it is real smoke or something else. It can be seen in Fig. 16 how the IR signals are affected less by the smoke particles.

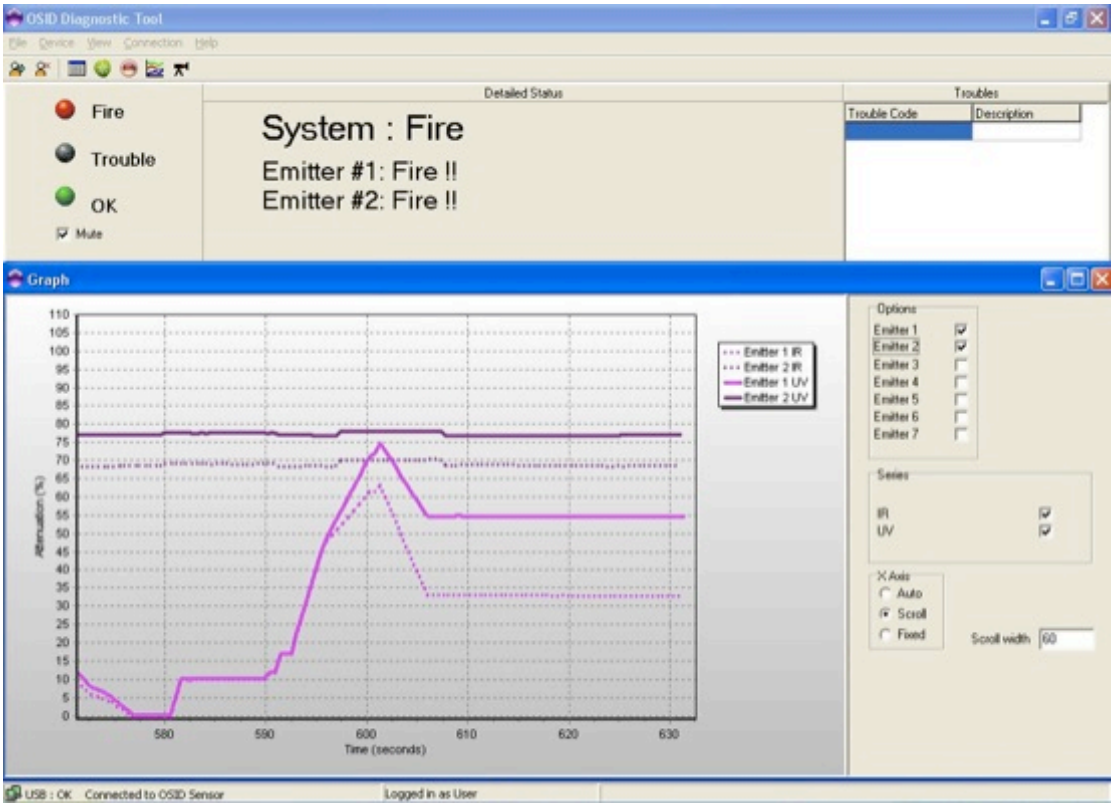

Figure 16: UV and IR signals of smoke in the Xtralis – OSID Diagnostic Tool

When the OSID imager detects smoke from any of the emitters associated to it, it raises an alarm and indicates from which emitter the detection was made. These alarm data are further used by the OSID 2-D Mesh to, additionally to detecting the presence of smoke, locate it within the covered area.

2.3.1 OSID 2-D Mesh

The detection and localization OSID-based system proposed in this thesis makes use of dual OSID measurements by taking the crossing points between two sets of emitters associated to two different imagers. Similarly to the 3-planar crossing points that form the FireCube in the multi-view framework, the linear detection readings from the OSID emitters associated to the two different imagers form, at

their crossings, the points of the OSID 2-D Mesh. A general example of an OSID 2-D Mesh in a square–shaped room can be seen in Fig. 17. In the example the symbols A_l and B_l correspond to the two imagers (i.e. imager A and imager B) while the symbols A_n and B_m correspond to the emitter number *n* or *m* associated to the corresponding imager. Each imager can have up to 7 emitters associated so *n* and *m* can be any number between 1 and 7. Then, given that all of the beams from one of the set of emitters cross the ones from the other (depending on the location of the detectors some beams would not cross all of the other imager's associated beams) the amount of crossing points, *CP*, is the product $CP = N \times M$, where *N* is the amount of emitters associated to imager A and *M* is the amount of emitters associated to imager B. Then, the maximum amount of points for an OSID 2-D Mesh is 49.

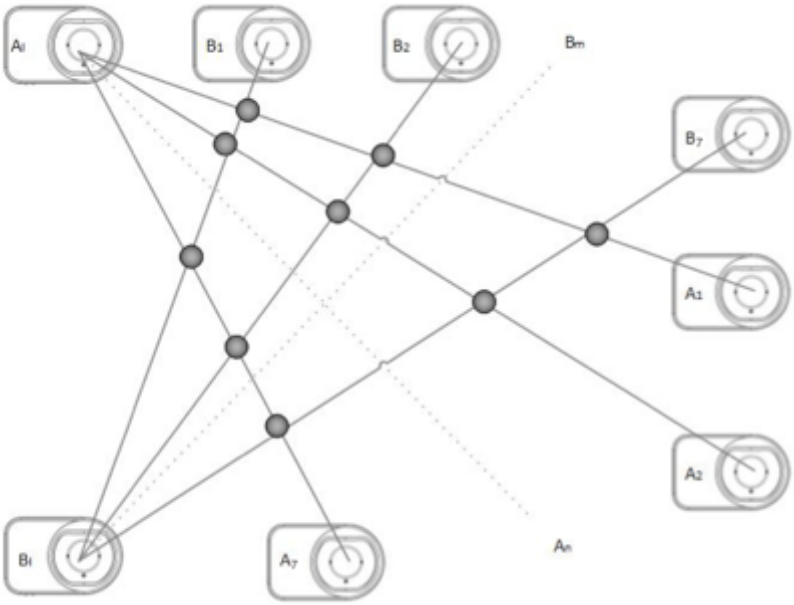

Figure 17: General example of OSID 2-D Mesh (top view)

The OSID 2-D Mesh is built within a reference coordinate system (e.g. 2-dimensional x-y) so every crossing point has an (x,y) coordinate. It is also possible to define a crossing point distance, $r_{cp}(n_1,m_1,n_2,m_2)$, corresponding to the distance between the crossing point of the lines of emitters n_1 and m_1 and the crossing point between the lines of emitters n_2 and m_2. This number can further be used to determine the reliability or 'extent' of the detection of a crossing point within the 2-D Mesh.

The information from the OSID detectors is used for confirming any initial detection alarm from the VFD. Furthermore, by implementing the OSID 2-D Mesh, the initial location of the fire can be determined and the spread of the smoke at ceiling level (at an initial state) can be traced, thus providing useful information for

the multi-view VFD framework. After receiving the alarm data from both imagers, either offline or real-time, and based on the input of the locations of the OSID detectors and the geometry of the place, the 2-D Mesh is created by the OSID Algorithm (Section 2.3.2) and the detection information is prepared for its combination with the multi-view VFD data.

2.3.2 OSID Algorithm

The OSID 2-D Mesh is created with the coordinates of the locations of the OSID imagers and their respective emitters and the information on the geometry (dimensions) of the covered area. Then, the detection input from the two imagers, as discussed in Section 2.1, is analyzed to determine which points of the 2-D Mesh are in alarm and when (for the offline case). For the work in this thesis the type of OSID detection data is the offline one. Thus, the CSV files with the emitter estates of both imagers are inputs for the algorithm. The aim of the algorithm is to create an output CSV file containing the exact time and date of one or several detections at crossing points in the 2-D Mesh and their x-y coordinates. This CSV file then works as an input for the VFD multi-view framework carrying out the combination of both systems.

A flowchart of the OSID Algorithm for detection and localization is shown in Fig. 18. The algorithm has two basic stages: the 2-D Mesh creation (left-side half of the diagram) and the detection analysis and output file creation (right-side half). During the 2-D mesh creation stage the algorithm calculates for every emitter (A_n), associated to the first imager (A_I), the equation of the line between it and the imager:

$$y = m_n x + b_n \tag{2}$$

where m_n is the slope and b_n is the constant of the line corresponding to emitter A_n. The coordinate system used is the x-y reference coordinate system discussed in Section 2.3.1. For each of the A_n, the algorithm verifies if there are crossing points with the lines formed between all of the B emitters and the B imager. Thus an equation similar to Eq. (2) is determined for each of the B_m where m_m and b_m are the slope and constant of the line corresponding to each emitter. The algorithm checks if the lines cross and, if they do, it verifies that the crossing point is within the covered area. If the crossing point is within this area, it is included in the 2-D Mesh. The process is done for every A emitter. When the 2-D mesh is constructed, the CSV sampled data log files corresponding to each imager are opened and read. For each of them, a list with any alarm status change (fire alarm, or fire out) is created, saving also the time and date values when these changes happen; these are the statusA

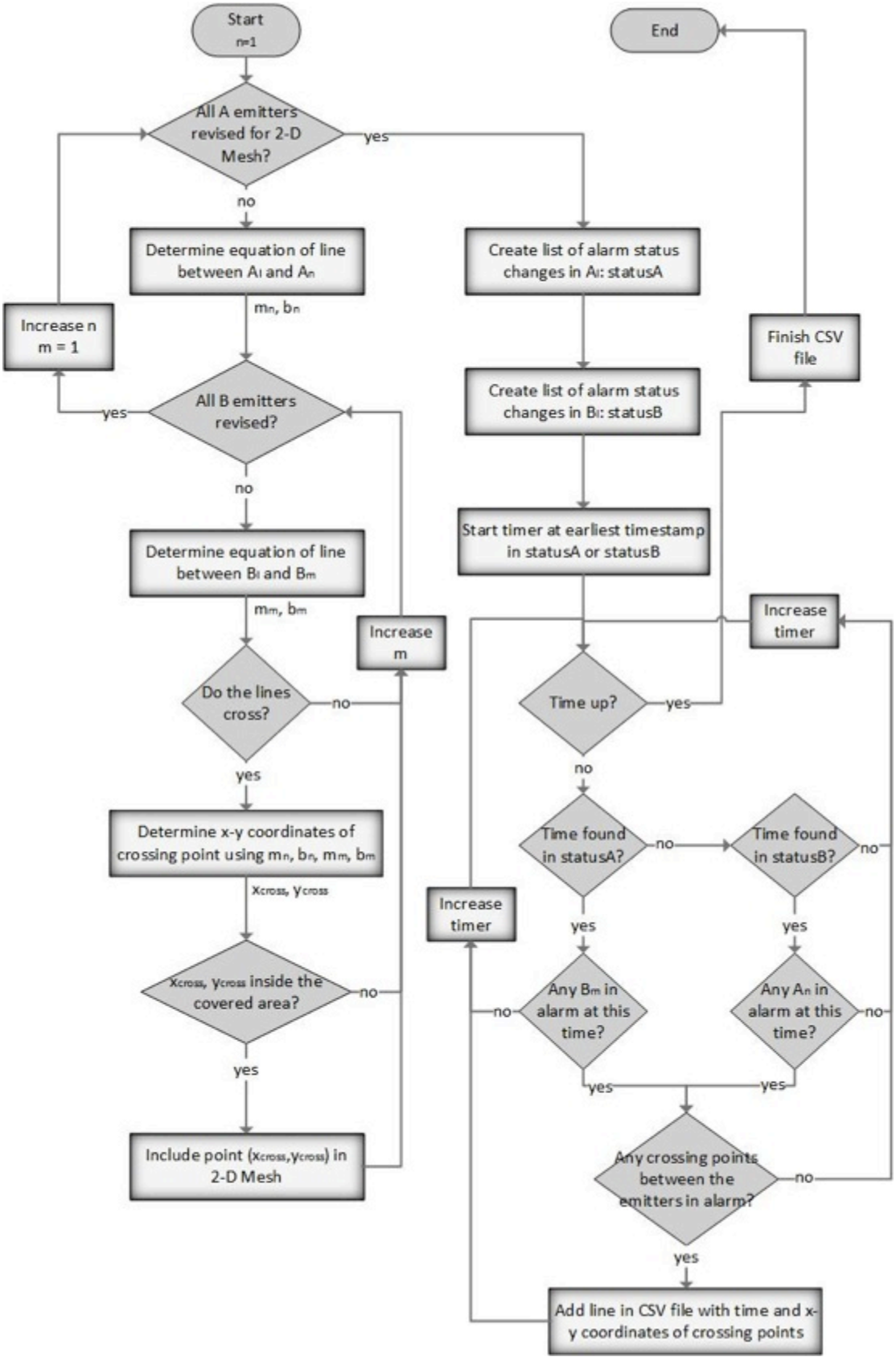

Figure 18: OSID Algorithm for detection and localization

and statusB lists. After creating the lists the algorithm starts a timer at the earliest time recorded in both lists and increases it second by second. For every step of the timer it is checked if any of the lists has an alarm status change at that time and, if so, it is checked on the other list if there are alarms present (i.e. based on the estate of the list just before this time step). If there are, the algorithm verifies if the emitters A and B in alarm have common crossing points in the 2-D Mesh. A new line with the value of the timer, and the corresponding x-y coordinates is added to the output CSV file if there are crossing points from the emitters in alarm. The process is repeated until the timer reaches the latest time recorded at both lists, when the CSV output file is completed.

A software tool was created for the implementation of the OSID Algorithm for Detection and Localization and its graphic user interface (GUI) can be seen in Fig. 19. It is through this interface that the inputs for the algorithm are entered. For this work, the areas covered by the VFD and OSID systems are rectangular, so the geometry of the room is entered by specifying its length and width. It is also necessary to know the locations of all the emitters and imagers, which are entered in terms of their x-y coordinates on the same reference coordinate system as the one used for the 2-D Mesh. Finally, the location of the CSV files corresponding to each of the imagers should be entered, so that the program can access the sampled data log. The output CSV file is saved in the same folder as the file corresponding to the OSID A and it is ready to be used as an input by the multi-view VFD framework.

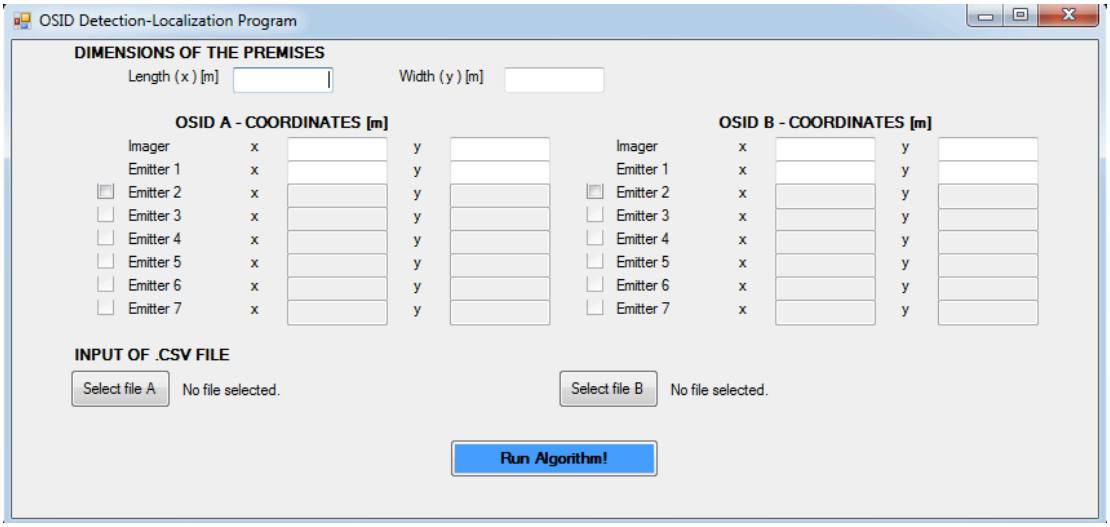

Figure 19: OSID program for detection and localization—Graphic User Interface

2.3.3 VFD-OSID Data Combination

There are two uses of the CSV file from the OSID program for detection and localization within the VFD multi-view framework. The first one is the modification of

the decision on the smoke-candidate points at the FireCube when the grid is analyzed. As discussed in Section 2.2, the FireCube is composed of the crossing points of the projection planes of the detection information from single-view VFD on a 3-D space. The analysis is done by taking the average of the P_{flames} and P_{smoke} of the point according to each of the planes that cross it and comparing it to predefined thresholds, as seen in Eq. (1). The first use proposed for the OSID data is the insertion of a fourth smoke probability value ($P_{smoke\text{-}OSID}$) based on the detection information from the OSID 2-D Mesh. By locating the FireCube point in the 2-D Mesh (i.e. its *x'* and *y'* coordinates), the fourth probability can be calculated based on the distance to the closest 2-D Mesh point in alarm, r_{alarm}, and to the closest 2-D Mesh point without alarm, r_{clear}, as follows:

$$P_{smoke,OSID} = \frac{r_{clear}}{r_{alarm}+r_{clear}} \tag{3}$$

This probability is a first geometric approach based on the weighed distance to the closest point in alarm and the closest point without alarm. As it can be noted, a FireCube point with a projection on the 2-D reference system having the same distance to the closest 2-D crossing point in alarm and the closest one without alarm would have a 0.5 probability of having smoke based on the OSID input. A point 10 times closer to the 2-D crossing point in alarm than to the crossing point without alarm would have a probability of 0.91 of having smoke. More complex probability calculations could be proposed, e.g. taking into account all of the 2-D crossing points with or without alarm surrounding the FireCube point in question. As mentioned before, this probability is to be averaged with the three probabilities from the sliced planes (two vertical and one horizontal) that cross at the specific point for the decision on which points of the FireCube are finally BG or FG points. Accordingly, the statement for the decision on the FG points in Eq. (1) is modified:

$$\text{FireCube}[x',y',z'] \rightarrow \begin{cases} FG, & \text{if } \overline{P_{flames}[x',y',z']} \geq t_{flames} \\ & \text{or } \overline{P_{smoke}[x',y',z']}' \geq t_{smoke} \\ BG, & \text{otherwise} \end{cases} \tag{4}$$

$$\overline{P_{smoke}[x',y',z']}' = \frac{P_{smoke,H}[x',y',z'] + P_{smoke,V1}[x',y',z'] + P_{smoke,V2}[x',y',z'] + P_{smoke,OSID}[x',y',z']}{4}$$

where, as it can be seen, the inclusion of $P_{smoke\text{-}OSID}$ can either lower down the average to correct a nuisance point or increase the average to correct a false negative.

The accuracy of the localization in the FireCube depends on the number of the horizontal and vertical planes and the spacing between them [23]. However, the more planes slicing the scene, the higher computational cost of the multi-view algorithm. So far, the multi-view framework works with uniformly spaced slice planes. The second use of the input data in the CSV file from the OSID program is,

then, using the detection data to determine in which areas it is important to have a higher accuracy (i.e. where there has been a detection from the OSID detectors). This way, a non-uniform plane slicing can be introduced, with more, closer planes where the OSID detectors have detected smoke and less, more spaced planes where there have not been detections. Because of the 2-dimensional nature of the 2-D Mesh, the planes of the FireCube that can have a non-uniform spacing are the vertical ones (i.e. the planes in the *x* and in the *y* direction). This concept can be compared to the non-uniform grid cells that can be used in the CFD Fire Dynamics Simulator (FDS) by NIST [24]. For the simulations performed using FDS, the default grid cells filing the computational domain are uniform in size but it is possible to make them non-uniform in up to two of the dimensions. The finer grid cells are also devoted to the most relevant regions or elements depending on what the aim of the simulation is. However, the non-uniform grid used in FDS is static throughout the simulation and, on the contrary, the proposed non-uniform plane slicing is dynamic. The time information attached to the 2-D Mesh detection is used to vary the amount and spacing of vertical planes of the FireCube with time. Thus, the non-uniform plane slicing can be better compared to the adaptive mesh refinement (AMR) carried out by other CFD simulators. AMR procedures require complex iterations as the desired grading of the mesh depends on the fluid flow itself, i.e. on the solution of the simulation [25]. For the proposed plane slicing the input is external, coming from the OSID detectors, so no iterative process is implied.

Section 2.3 has been dedicated to the description of the OSID-based smoke detection and localization scheme, i.e. the OSID 2-D Mesh, and of its output data which is used as an input to the VFD multi-view framework. The two uses of the data discussed reduce the amount of false positives or negatives of the multi-view framework and help in the optimization of the usage of computational resources. OSID detectors can also be combined with the multi-view VFD framework in the determination of the smoke layer height, as described in the following section, providing useful information for fire forecasting.

2.4 Smoke Layer Depth Measurement

The smoke layer has a fundamental connection to life safety during a fire as, firstly, the radiation from the hot gases to the people can cause dangerous burns and the inhalation of combustion products can be fatal and, secondly, the temperatures attained in the regions in contact with structural members and masonry can make these fail thus blocking evacuation paths (or access for the fire service) or even killing people. The first two of the mentioned hazards of the smoke buildup are related to the closeness of the smoke to the people and that is why tenability limits during a fire are often defined in terms of (or related to) the depth of the smoke

layer. Also, the smoke layer depth and growth rate are related to the mass flow from the buoyant plume into it, which is related to the dimensions of the plume and fire. Therefore, the knowledge of the smoke layer depth results useful for both, the determination of tenability limits and for fire forecasting (Section 1.1.3).

The VFD multi-view framework makes use of an adaptive bounding box algorithm to determine which of the detected points in the FireCube correspond to the smoke layer, as discussed in Section 2.2. By retrieving separate plume and smoke layer boxes, the depth of the smoke layer can be known at every analyzed frame by measuring the depth of its corresponding box. For the measurement with the OSID detectors, these are distributed in a vertical way, in the form of an array of emitters and their detection data is processed and prepared for its usage as an input by the VFD framework, in a similar way as with the detection and localization data, as described in the following sections.

2.4.1 *OSID Set-up*

Unlike the set-up for the smoke detection and localization with OSID (i.e. the 2-D Mesh) in which two different sets of OSID detectors were used in a horizontal, 'planar', configuration, for the measurement of the smoke layer depth only one set of OSID detectors is used. The emitters are placed vertically in a linear configuration forming an array of OSID emitters—the OSID Array. All of the emitters of the OSID Array are associated to one same imager (placed in a different wall) as shown in Fig. 20. As seen in the figure, the first of the C_k (the emitters in the array) is the top one. The reference system for the location of the OSID detectors is based on the ceiling and the symbol z_k represents the distance between the ceiling and the k-th emitter. The imager, C_I, should be located as low or lower than the last of the emitters in the OSID Array, i.e. the bottom one, (that is $z_I \geq z_K$ with K = total number of emitters, $1 \leq K \leq 7$) so that the interruption by smoke of the signals between the imager and the emitter happens at the height of each emitter. The measurement of the smoke layer depth is done, thus, based on the location (height) of the emitters that go in alarm: the lowest of the emitters in alarm determines the measured depth. Consequently, the growth of the smoke layer is not recorded continuously but rather discretely, at the measuring heights that correspond to the C emitters locations. Also, the accuracy of the information is related to the closeness of the emitters. The minimum distance at which they must be installed is not specified by Xtralis and it rather depends on the distance to the imager (i.e. the farther the imager is installed the more spread apart the emitters should be). For the work on this thesis it was tested, though, that a spacing of the emitters of 0.3m was detectable by an imager 10m away. As it can be deduced from Fig. 18, the deepest smoke layer that the OSID Array can record corresponds to a layer with a depth of z_K.

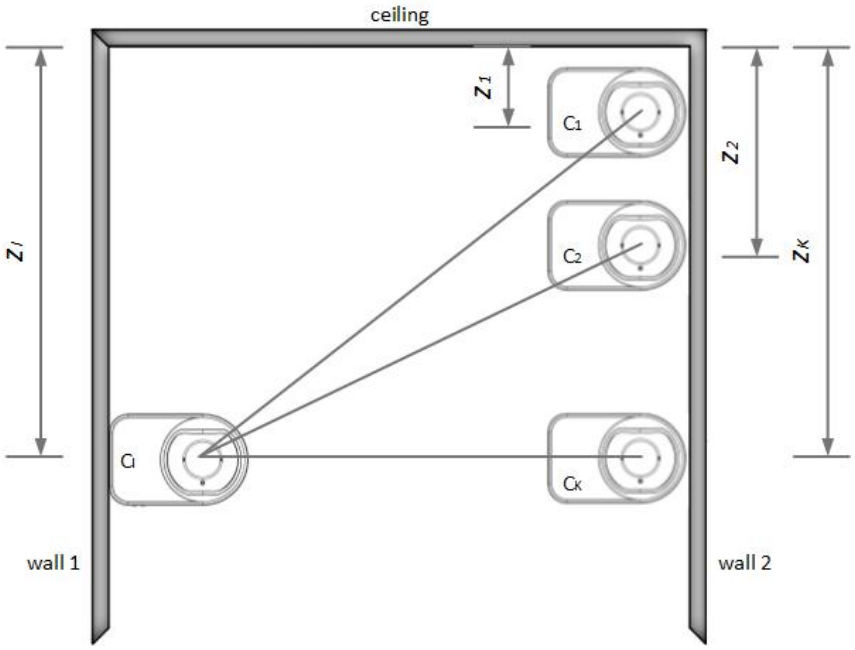

Figure 20: General OSID Array for smoke layer depth measurement

2.4.2 *OSID Algorithm*

The smoke layer depth information from the OSID Array is also prepared as a CSV file to use as input for the VFD multi-view localization framework. It is based, too, on the alarm information from the OSID detectors, in this case from the C imager. For this thesis, the algorithm for creating the output CSV file is based as well on the offline information in the CSV sampled data log file from the Diagnostic Tool. A flowchart of the OSID Algorithm for smoke layer depth measurement can be seen in Fig. 21. As for the smoke detection and localization algorithm, the inputs are the location of the OSID detectors, the geometry of the place and the CSV log file. The difference is that the location of the OSID detectors and the geometry of the place are given in one dimension (i.e. the z_I, the different z_K and the height of the ceiling).

As it can be noticed from the figure, the algorithm is simpler in this case. First, a list is created with the distances from the ceiling of all of the emitters, z_k. It can be noted that the location of the imager, z_I, is not taken into account in the algorithm; the requirement is that it is not placed higher than any emitter of the OSID Array. Similarly to the smoke detection and localization algorithm, a list of alarm status changes (statusC) is created, and a timer is started at the earliest of the times of the events recorded in this list. The algorithm is run until the timer exceeds the time corresponding to the last event recorded in statusC. For every incremented second of the timer, the new time is searched in the events in statusC and, if found, the emitters in alarm in the corresponding event are evaluated. The maximum value z_k of the emitters in alarm will be taken as the new smoke layer depth and the

output CSV file will be updated with a new line including the time and the smoke layer depth, z_{layer}. When the timer reaches the final time, the file is completed.

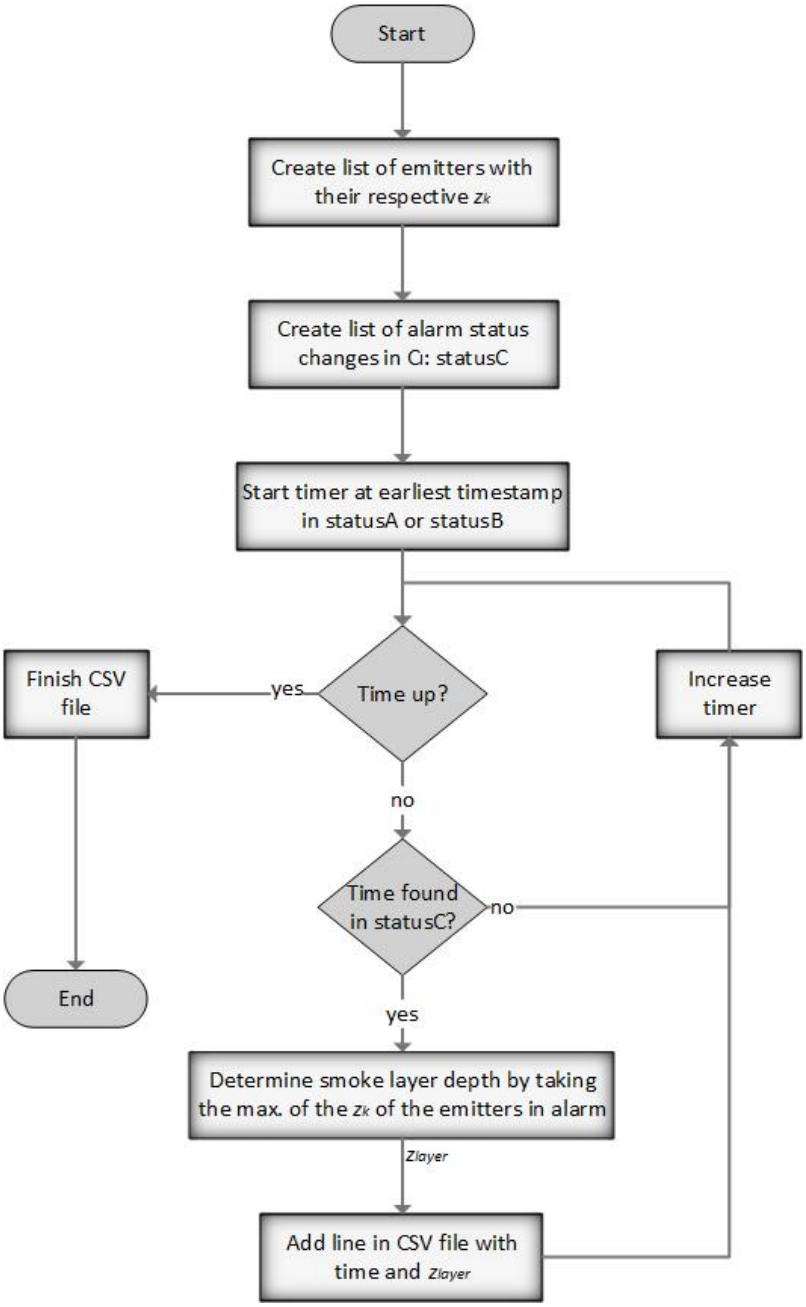

Figure 21: OSID Algorithm for smoke layer depth measurement

Similarly to the case of the detection and localization algorithm, a software tool was created to implement the OSID Algorithm for smoke layer depth measurement and its GUI can be seen in Fig. 22. In this case, it only requires one dimension of the place (the height), the heights of the OSID detectors (expressed as

distance from the ceiling), and just one input CSV log file. The output CSV file is further used by the VFD multi-view framework for combining the data from both the VFD and the OSID.

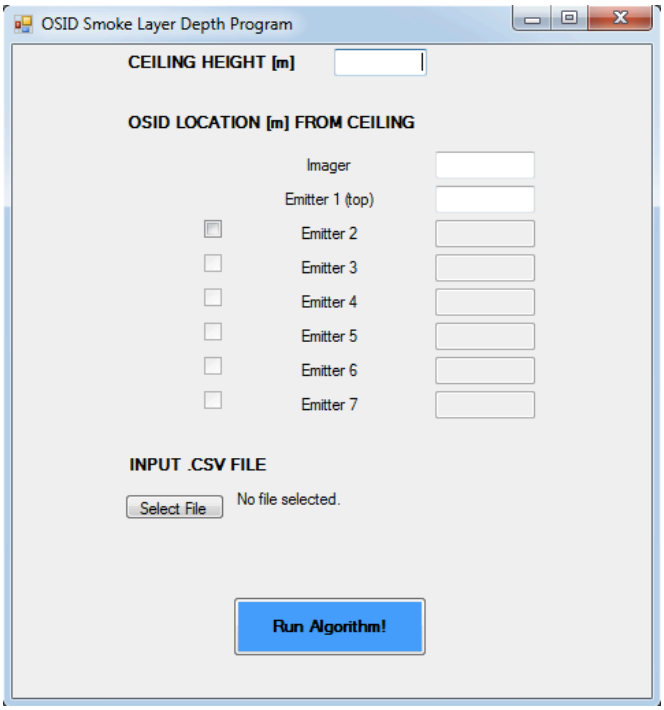

Figure 22: OSID program for smoke layer depth measurement—Graphic User Interface

2.4.3 *VFD-OSID Data Combination*

The smoke layer depth is retrieved by the VFD framework at every time by measuring the depth of the smoke layer bounding box in the FireCube. With the information from the CSV file from the OSID Algorithm for smoke layer depth measurement, the depth of the bounding box can be verified and corrected if necessary. As mentioned in the previous section, the CSV file from the OSID Algorithm includes rows of events corresponding to when there is a new alarm change in the C imager (e.g. a new emitter is in alarm or an emitter stopped being in alarm). Each row contains the time (and date) of the new status change and the corresponding smoke layer depth at that time. Clearly these represent discrete smoke layer depth values, so the values corresponding of the times in between should be estimated. As a first approach, a linear interpolation between each pair of values is proposed. Then, for an example of an OSID Array of 4 emitters spaced 40cm from each other (and from the ceiling) detecting smoke at 40, 70, 90, and 100 seconds respectively, the continuous values of the smoke layer depth would be as shown in Fig. 23. More complex calculated values could be obtained by taking into account the rate of growth of the smoke layer according to previous points.

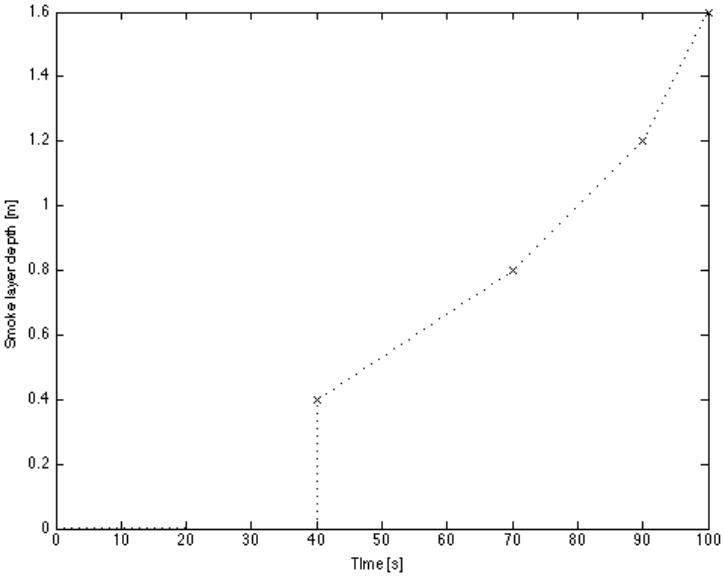

Figure 23: OSID smoke layer depth linear interpolation

The VFD multi-view framework determines the size of the smoke layer box in the FireCube with the adaptive bounding box algorithm, as described in Section 2.2. Accordingly, an upper box containing 10% or less background points is taken as the smoke layer box. The proposed combination with the OSID input takes into account the measured (and calculated) smoke layer height from imager C, z_{layer}. Then, the iterative process of the bounding box algorithm does not only analyze the percentage of BG points inside the box to decrease its vertical dimension in the upward direction, but it also checks on the value of z_{layer}. Only if both conditions, having more than 10% of BG points and having a depth greater than z_{layer}, are satisfied the depth of the bounding box will be reduced. With this combination of the VFD and OSID measurements, any missed detection by the VFD will be corrected by the OSID information.

2.5 OSID-VFD Experiments

The OSID set-ups described in sections 2.3.1 and 2.4.1, i.e. the OSID 2-D Mesh and the OSID Array, were tested during the course of this thesis in the construction were the Fire Safety and Explosion Safety in Car Parks [26] project took place. This car park in WarringtonFire Gent (the top view of the drawing shown with a transparent roof in Fig. 24) has wide enough dimensions, 28.6m x 30m, for deploying a 2-D mesh. Although it is only 2.8m high, it is also possible to install an OSID Array starting close to ceiling level, and work with it as if it were installed in a higher place. Given these possibilities, two sets of experiments were planned: one for smoke detection and localization and another for the smoke layer depth measurement. It was planned to

do the experiments in the back part of the car park, delimited by the dashed line in the figure. The aim was to implement and test in "real-scale" conditions both of the OSID set-ups described in this thesis. Also, VFD sensors were installed to have detection information from a common scene from both, the VFD multi-view algorithm and the OSID algorithms[2]. Then, for all of the experiments both OSID detectors and VFD video cameras were used, all monitoring the same reference area. The first set of experiments was the one for smoke detection and localization.

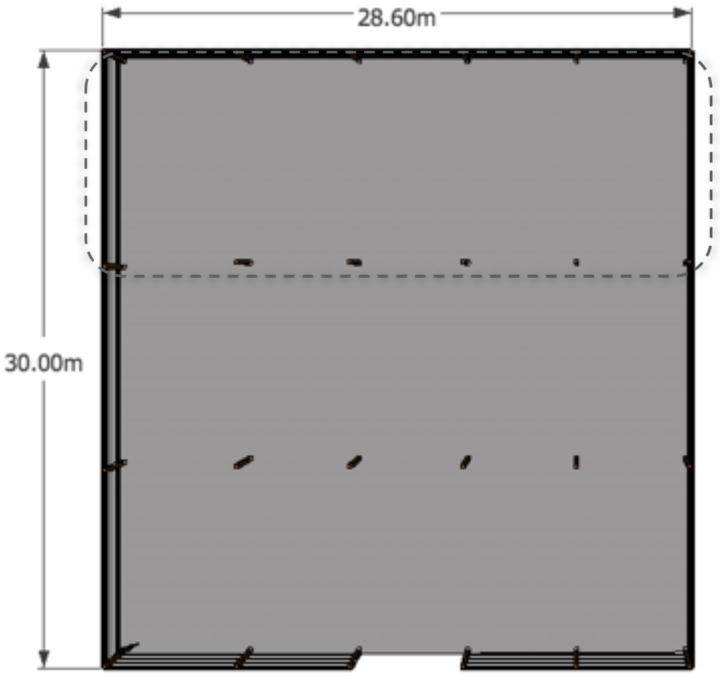

Figure 24: Car park in WarringtonFire Gent (Drawing—Top View)

2.5.1 Smoke Detection and Localization

For the smoke detection and localization experiments, three VFD cameras and a 2-D Mesh including two OSID imagers and six emitters were used. The scene that was to be monitored is delimited by the dashed line in Fig. 25. The chosen positions for the VFD sensors can also be seen in the figure. It should be noted that the two cameras to the left side of the figure are enough to create a FireCube covering a region past the right border of the area inside the dashed line; that is, the third camera is not necessary for the multi-view algorithm to work and it is used for improving the accuracy, as mentioned in Section 1.1.2. The location of the OSID detectors in the 2-D Mesh was chosen so that most of the crossing points would fall inside the area of

[2] In this thesis only the VFD information of the smoke layer depth experiments is included. The information of the first experiments will be further retrieved and analyzed.

the fire scene. The locations, the detection lines (beams), and the resulting 2-D Mesh are also shown in Fig. 25. As it can be seen in the figure, all of the beams cross each other so the number of crossing points is 9, and 7 of them are within the area of the fire scene.

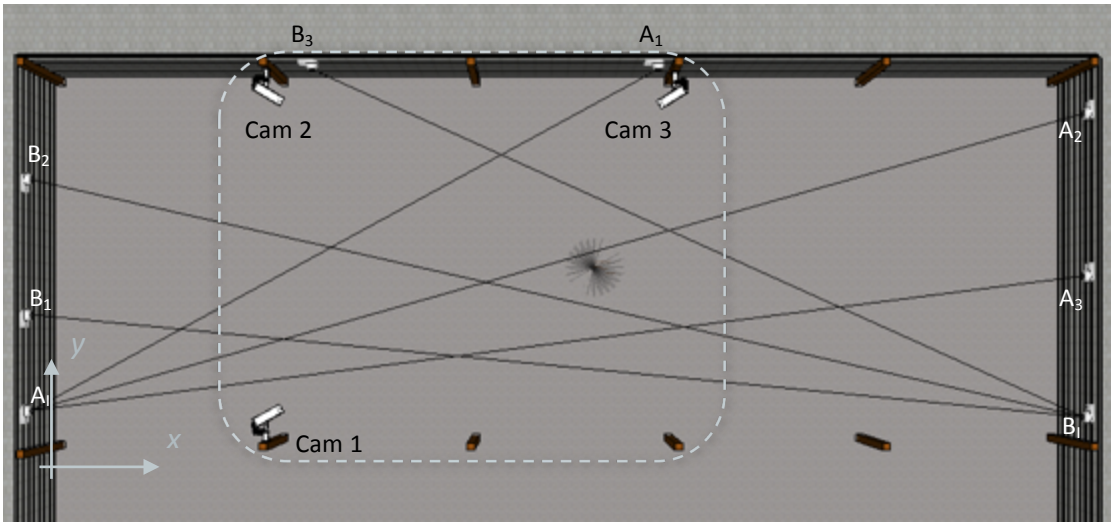

Figure 25: OSID 2-D Mesh and VFD sensors for smoke detection and localization experiments

The coordinates of the horizontal-planar locations of the OSID detectors and VFD cameras (numbered clockwise starting from the lower one in the figure) are listed in Table 1. For ease during the installation of the OSID detectors, the initial exact locations were slightly varied, however Table 1 contains the coordinates actually used. The materials planned for the experiments included fast burning ones like (dry) Christmas trees and straw and smoldering ones like wood. This way, the detection time could also be tested. It was also planned to do some experiments burning printed paper/magazine paper. A total of 10 experiments were carried out, with either of the mentioned fuels and at different locations within the region delimited. The specific locations of all of the fires and the results of the measurements from the OSID 2-D Mesh and the FireCube can be found in Chapter 3.

Table 1: OSID detector and VFD camera location for the smoke detection and localization tests

Device	Location	
	x [m]	y [m]
Imager A	0	0.4
Emitter A1	16.7	9.95
Emitter A2	28.6	9.16
Emitter A3	28.6	4.36
Imager B	28.6	0.25
Emitter B1	0	2.3
Emitter B2	0	7.3
Emitter B3	6.9	9.95
Camera 1	6.5	0
Camera 2	6.5	10.12
Camera 3	17.6	10.12

2.5.2 *Smoke Layer Depth Measurement*

A second set of experiments was planned for the smoke layer depth measurement system. In this case, an array of 5 OSID detectors was constructed and a wall was built to contain most of the smoke produced and, thus, facilitate the buildup of smoke into an observable layer. As explained in Section 2.2, the way of retrieving the smoke layer depth from the multi-view VFD algorithm is creating a separate bounding box for the smoke layer and another one for the buoyant plume. By measuring the depth of the smoke layer bounding box, the value of z_{layer} is retrieved. However, given that the experiments in this thesis are not testing the actual combination of the OSID Systems with the VFD multi-view framework, a simpler, visual single-camera VFD approach was used for the smoke layer depth measurement. This VFD approach is based on the energy content of predefined lines in the video frames [3]. Thus, two cameras were installed, one above the other, to record the video needed to run the visual VFD approach (the videos from the two cameras were independent, the second camera used for comparison). The new wall and the location of the OSID Array, of the C Imager, and of the VFD sensors are shown in Fig. 26. In the figure it can be seen one camera covering the other.

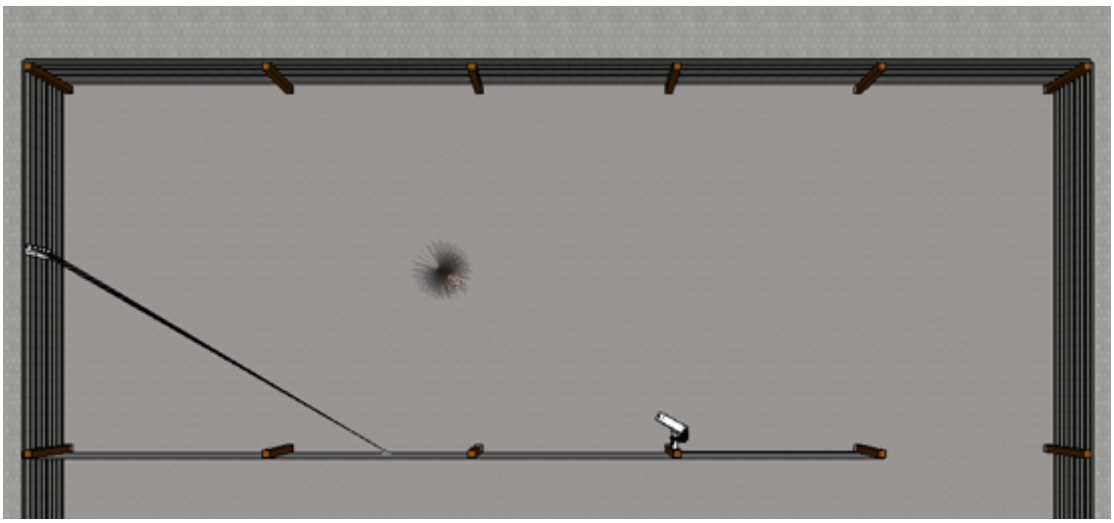

Figure 26: OSID Array (detailed view in Fig. 27) and VFD sensors for smoke layer depth measurement experiments (top)

It was planned to place the OSID Array close to the ceiling so the first emitter, C_1, was placed 10cm from it. The other four emitters from the array were placed at equal distances of 30cm from each other. The whole OSID Array, constructed in a board of Promatect, had a total length of 1.5m. The different distances, z_k, from the ceiling to the emitters in the array are listed in Table 2 and a 3-dimensional view of the drawing with the set-up can be seen in Fig. 27 with the location of the C imager and the OSID Array.

Table 2: OSID array distances from the ceiling for smoke layer depth measurement experiments

Device	z_k [m]
Imager C	1.3
Emitter C1	0.1
Emitter C2	0.4
Emitter C3	0.7
Emitter C4	1
Emitter C5	1.3

The materials planned to burn for these tests were straw and paper regardless of the speed of burning; this because the aim of the fires was to get the smoke for the buildup of the smoke layer rather than testing any detection speed. There were a total of three experiments performed with the results for both, the OSID system and the VFD system, presented in Chapter 3.

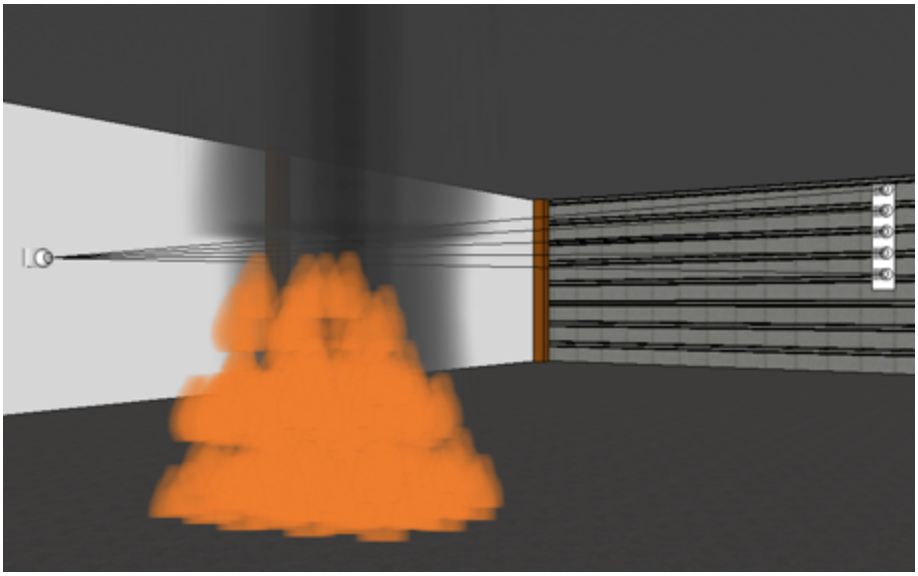

Figure 27: OSID Array and imager for smoke layer depth measurement experiments (isometric)

3. Results

The two sets of experiments performed to test the OSID set-ups introduced in this work (i.e. the OSID 2-D Mesh and the OSID Array) were carried out in the car park in WarringtonFire Gent where the Fire Safety and Explosion Safety in Car Parks [26] project took place, as mentioned in Section 2.5. As explained, both sets of experiments were performed with different configurations of the car park. That is, for the smoke layer depth measurement experiments an additional wall was built to contain the smoke in a smaller region. The measurements done by the corresponding OSID systems, the measurements done by the VFD system in the smoke layer depth measurement experiments, and all of the information collected from the experiments is presented in this chapter. The results from the smoke detection and localization experiments are first presented with the ones from the smoke layer depth measurement experiments following.

3.1 Smoke Detection and Localization Experiments

For the smoke detection and localization experiments an OSID 2-D Mesh consisting of 2 imagers, with 3 emitters each, was deployed. Also a VFD system consisting of 3 (visual) video cameras was installed. As mentioned in Section 2.5.1, a set of 10 experiments were performed by burning dry Christmas trees, straw, paper and wood. The different locations and types of fuels used in each of the experiments are listed in Table 3, the coordinate system being the same used for the location of the OSID detectors in Table 1 (which was also used for the 2-D Mesh). The fuels were located at points close to the center and the middle-rear part of the fire scene (region inside the dotted line in Fig. 25) so that the crossing points were more spaced. This way there was a higher probability that the smoke would take longer in being detected by a crossing point and the “slow case” detection time could be measured (as a worst-case approach opposed to the closer crossing points were detection could be done faster) for the OSID 2-D Mesh.

Table 3: Smoke detection and localization experiments – Location and type of the fuels

Test	Fuel	Location	
		x [m]	y [m]
1	Christmas tree	12	3.8
2	Christmas tree	12	6.5
3	Paper (inside metallic bin)*	13.75	6.25
4	Straw	12	6.5
5	Paper (inside metallic bin)*	12	3.8
6	Baskets and wood	12	3.8
7	Wood Sticks (on electric burner)	12.6	5.1
8	Wood Sticks (on electric burner)	12.7	2.5
9	Paper (inside cardboard box)	12	6.5
10	Christmas tree	9	7

A picture of the first experiment (Test 1) is shown in Fig. 28. In the figure it is possible to see the video sensor Cam 1 and the OSID detectors A_I, B_1, and B_2, in order from left to right. It also shows a Christmas tree, which was located 12m horizontally and 3.8m vertically from the coordinate reference origin as seen in the first row in Table 3. It should also be noted from the table that tests 3 and 5 have (*) symbols, which mean the fuels were placed to produce extra smoke for the previous experiments, respectively. However, the differentiation between tests 2-3 and 4-5 is mainly done in the VFD algorithm.

Figure 28: Smoke detection and localization experiments – Christmas tree

3.1.1 OSID 2-D Mesh

As previously mentioned, the detection and localization information retrieved from the VFD algorithm is not included in this thesis. From the OSID system, on the other hand, the 2-D Mesh output and the detection times (seen in Table 4) were retrieved.

Table 4: Smoke detection and localization experiments – OSID detection time after ignition

Test	Detection Time OSID [s]	Detection Time 2-D Mesh [s]
1	18	23
2	14	25
3	-	-
4	3	36
5	-	-
6	31	69
7	62	74
8	142	163
9	5	5
10	5	13

Two types of detection times were measured, both after the moment of ignition of the fuels. The OSID detection time refers to the time spent until the first OSID emitter detects smoke. The 2-D Mesh detection time refers to the time when there is a detection by a crossing point (i.e. when the smoke is first localized). From the table it can be already seen that the cases with a smoldering fuel (i.e. wood) took the longest time to be detected. It can also be seen that there is a delay in the 2-D Mesh detecting its first point, which is related to the time it took for the crossing emitter to detect the smoke. As stated before, the differentiation between tests 2-3 and 4-5 was mainly done in the VFD algorithm, and for the OSID systems they acted like single tests with two 'peaks' of smoke. That is the reason why there were no detection time measurements for tests 3 and 5. For each of the remaining tests the location of the fuel and the location of the first detection point from the 2-D Mesh are plotted in Fig. 29. As discussed in Section 2.3.2, the CSV output file from the OSID Algorithm for smoke detection and localization contains lines with the progress of the 2-D Mesh detection points; that is, the different moments in time in which new crossing points raise alarms or go back to normal status. The figure shows the first detection points at each of the tests thus the corresponding time of detection is the one listed in the third column in Table 4.

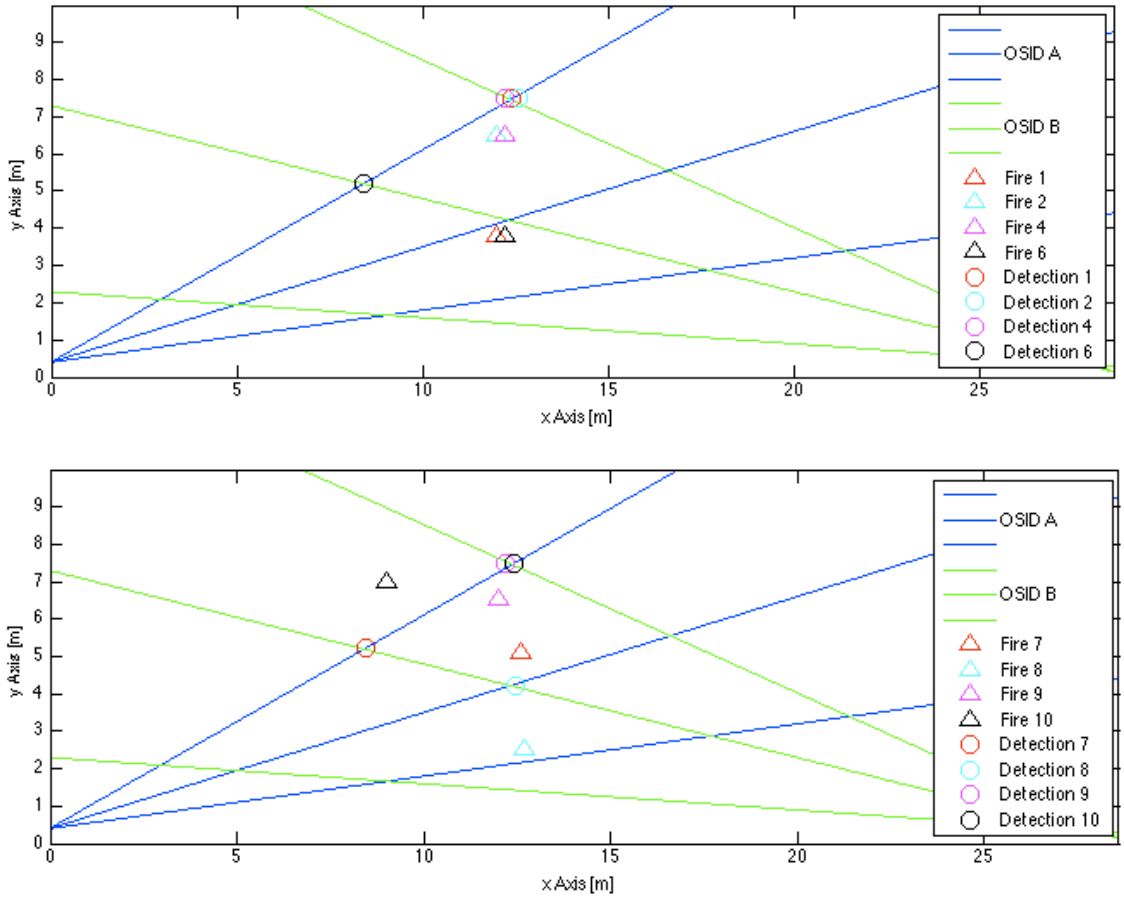

Figure 29: Smoke detection and localization experiments – 2-D Mesh detections

The contents of the output CSV files from the smoke detection and localization algorithm are included in Appendix 1, where they have been organized as a table (i.e. each comma represents a new column). As explained in Section 2.3.2, each line includes the exact time and date, the number of detected points and their corresponding x-y coordinates. It can be seen from the files how the smoke is spread from being detected at a single crossing point until it covers all of the 9 crossing points. Some lines with 0 detection points can also be found, which mean that there was a detection by a single OSID (e.g. the initial detection) or that an OSID that was detecting smoke without crossing any other emitter went normal (e.g. the last emitter to go to normal status). Then, as it can be inferred, each of the "sets of status changes" (i.e. starting with 0 and ending with 0 detected points) represents one of the tests performed. For example, the first experiment (test 1) corresponds to the lines between 13:34:02 and 13:34:55. The first line of the file, then, corresponds to the first detection of a single OSID for test 1, and the second line corresponds to the initial 2-D Mesh detection, which is the point plotted in Fig. 29 (x=12.4, y=7.49 in red in the top graph). The same applies to the other experiments.

It is possible to observe the evolution of the smoke through the crossing points of the 2-D Mesh based on the detections from the CSV output file. Fig. 30 shows an example for test 1. As it can be seen in the figure, the first crossing point to detect was the one at x=12.4, y=7.49, also plotted in Fig. 29. The detections that follow in time correspond to the same point x=12.4, y=7.49 and the new x=12.4, y=7.49, 49s after ignition (in cyan in the figure). Similarly, the rest of the points are plotted in the figure, with the color indicating at which time (expressed in seconds after ignition) the 2-D Mesh detections happened. This way, it is possible to know the behavior of the smoke (at the initial stage of the fire).

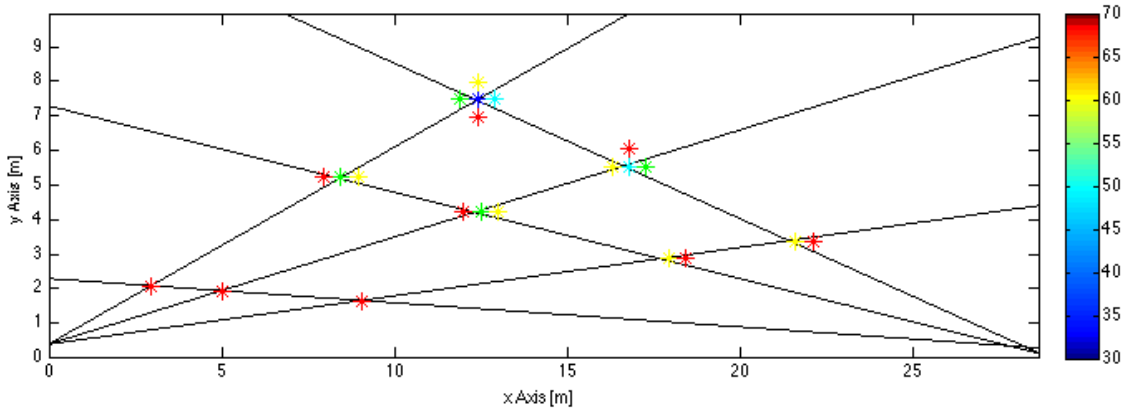

Figure 30: Smoke detection and localization Test 1: 2-D Mesh detections with time (color bar represents time after ignition [s])

3.2 Smoke Layer Depth Measurement Experiments

The second set of experiments performed in the car park was for the smoke layer depth measurement. As mentioned in Section 2.5.2, an OSID Array of 5 emitters associated to one imager and 2 VFD cameras were used for these three experiments. Also, the materials used as fuels were straw and paper. However, the type of fuel was not taken into account as long as there was enough production of smoke for the buildup of a smoke layer. A picture of the actual setup in the car park for the first test is shown in Fig. 31. As it can be seen in the figure, a wall was built to retain the smoke from spreading in all of the car park and having a faster, easier, buildup of smoke in the fire scene chosen.

Figure 31: Smoke layer depth measurement experiments – Straw

3.2.1 OSID Array

The OSID Array used for the experiments is shown in Fig. 32. As mentioned in Section 2.5.2, the emitters from the array were spaced 30cm from each other, and the first one (i.e. C_1) was placed 10 cm below the ceiling. The readings of the OSID detectors from the array were used by the algorithm for smoke layer depth measurement to calculate the value of z_{layer}. The CSV output file can be found in Appendix 1 (last table), where it has also been formatted to look like a table. The corresponding plots against time (after ignition), using the linear interpolation proposed in Section 2.4.3, are presented in Fig. 33, where the OSID-based smoke layer depth has been plotted together with the output from the VFD algorithm.

Figure 32: Smoke layer depth measurement experiments – OSID Array

3.2.2 VFD

The VFD sensors used for the smoke layer depth measurements were two (visual) video cameras. As mentioned in Section 2.5.2, the VFD algorithm to be run for these specific tests was not the one corresponding to the multi-view framework but a single-view approach based on the energy contained in predefined lines of the video frames. There were two lines predefined for each camera, so there were 4 values available at every moment of the tests (i.e. that could be compared to each other). These values were averaged to have only one (instead of 4) smoother plot of z_{layer} to compare to the output from the OSID algorithm. The two plots of z_{layer} for each of the tests are shown in Fig. 33. The figures do not include the whole duration of the experiments as the smoke layer depth information from the VFD algorithm became invalid once the cameras got surrounded by smoke, which happened by the last part of all of the tests. The non-averaged smoke layer depth calculated with each energy line of each camera is included in Appendix 2. The corresponding values obtained from the OSID algorithm are also plotted. It was observed during the experiments that the first and second tests (using straw) produced abundant, thick smoke while the third one (using paper) produced less and lighter smoke. This can be confirmed by looking at the corresponding plot in Appendix 2, where there is greater noise and less similarity between the VFD-based smoke layer depth values.

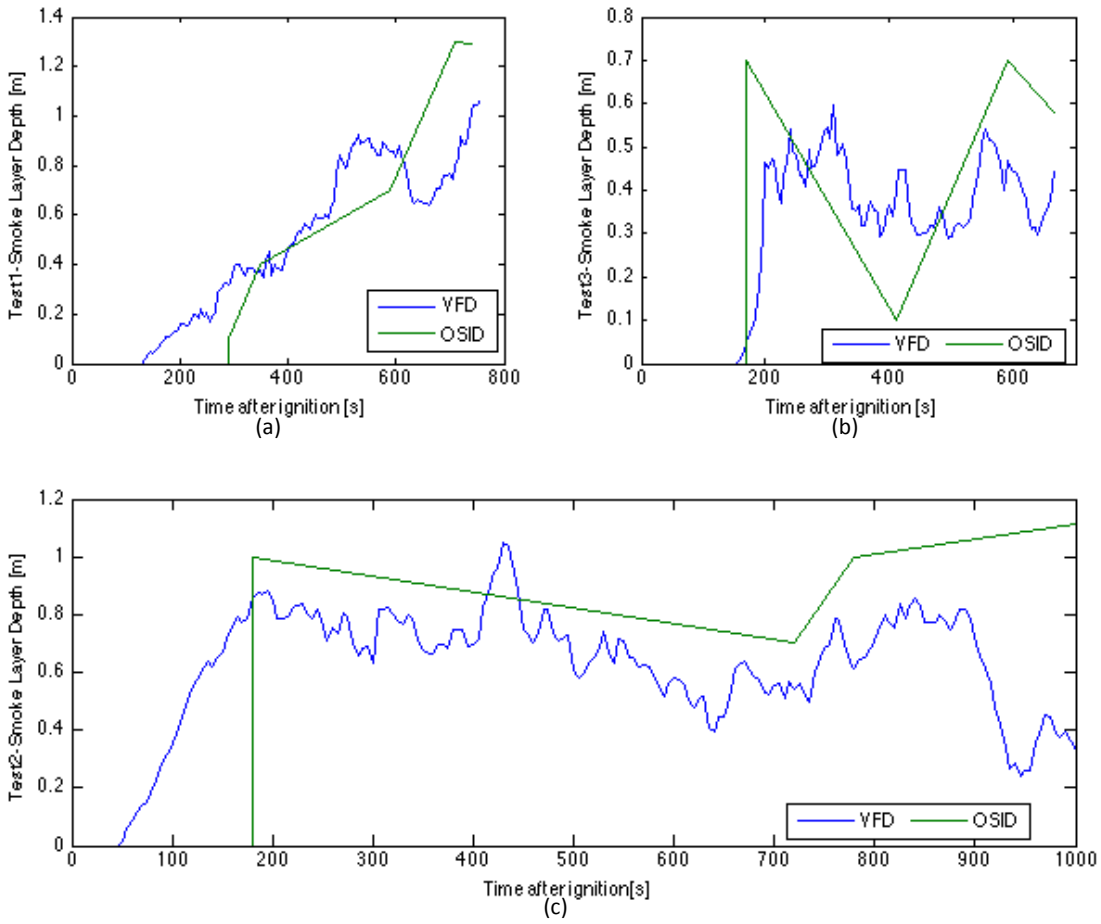

Figure 33: OSID-VFD smoke layer depth measurement readings: (a) Test 1, (b) Test 3, (c) Test 2

4. Discussion

The measurements and observations from the two sets of experiments with the OSID-based systems introduced in this thesis were presented in the previous chapter. As mentioned, the purpose of the experiments was to test the two systems with smoke produced by real fires. It was also aimed to check the coherence of the outputs form each of the algorithms. In this chapter, the measurements obtained by the OSID sensors are analyzed based on the known ground-truth of the experiments (e.g. the ignition time and the location of the fuel). It finalizes with a section on further approaches based on the global objective of the combination of VFD systems with volume sensors and on the work covered by this thesis.

4.1 Smoke Detection and Localization

The output from the OSID-based system for smoke detection and localization, i.e. the 2-D Mesh, is the CSV file with the coordinates of the different crossing points in alarm at given time stamps during the fire. It is difficult to have the *exact* ground-truth of the smoke behavior and spread but, as a basic evaluation of the system, it is possible to analyze the accuracy of the first detected crossing point by comparing it to the location of the fuel and it is also possible to compare the initial time of the alarm (of both the first single emitter and the first crossing point) to the ignition time. In Table 4, both of these times have been compared and their difference (i.e. the detection time) is listed. Based on the type of fuel of each test from Table 3, it can be seen that the shortest detection times were obtained for the experiments with Christmas trees, straw and paper. These correspond to the experiments with fastest burning and more smoke produced. The single-OSID detection time is always equal to or less than 18 seconds showing the fast response of the OSID detectors. However, as it can be observed from the table, the detection time of the first 2-D Mesh point to alarm has an additional delay. For this first crossing point to trigger an alarm it is necessary that two crossing emitters detect smoke, thus the detection times from both affect the detection time of the 2-D Mesh. A coarser 2-D mesh will probably have greater delays between a single OSID detecting and the 2-D Mesh detecting. Thus, it will always be important to keep the single-OSID reading (i.e. its conventional use as a beam detector). Then, it is clear that the detection time of the proposed system will not be better than the detection time of a single OSID and, on the contrary, it introduces a delay time which can be zero (as in the case of test 9) or can be considerably longer (as in test 4) depending on the configuration and spacing of the mesh.

The location of the first detection by the 2-D Mesh was expected to be at the crossing point closest to the fuel being burned. However, as it can be observed in Fig. 29, it was not always the case. For an ideal case it would have been true, as the fire plume would have risen in a straight way and spread radially from the coordinates corresponding to the location of the fuel. However, the air movement in the car park made the smoke plume not be symmetric and incline as it is shown in Fig. 34. The considerable horizontal air velocity was a result of the big opening on the front wall of the car park, which can be observed on the bottom of Fig. 24.Thus, it is noticeable that the accuracy of the localization of the initial fire based on the 2-D Mesh readings (i.e. the coordinates of the first crossing point to detect) depend on the conditions of the air velocity at the place in addition to the coarseness of the mesh. Nonetheless, the system detected and followed the movement of the smoke, providing its spread behavior at the early moments of the fire, as it was expected to.

Figure 34: Smoke detection and localization experiments – Paper in metallic bin

4.2 Smoke Layer Depth Measurement

The main parameter for the smoke layer depth measurement experiments was z_{layer}. As discussed in Section 2.4.1, z_{layer} measured by the OSID array will have as many possible values as emitters in the array. From the experiments (and from Fig. 23), it can be seen in Fig. 33 that the initial growth of the smoke layer is not measured or estimated by the system, thus having an initial gap in the information. Also, based on the plots of the VFD results on the figure and given the 30cm-sensitivity of the implemented OSID array, it can be said that both systems followed similar trends. Taking the VFD readings as the closest available to the ground-truth, the results from

the OSID-based system are agreeable. However, when combining the VFD systems with an OSID Array it would not be advisable to use all of the detected/estimated values but only those exceeding the smoke layer depth calculated with the VFD, as done by the decision discussed in Section 2.4.3 (i.e. that the adaptive bounding box is only contracted if there are more than 10% BG points inside and if the its depth is greater than the OSID-based value). This implies a conservative decision when taking into account the input from both systems.

The smoke layer experiments also showed how the VFD sensors malfunction when immersed in smoke. This fact is the reason why the plots from Fig. 33 do not show the whole tests, i.e. the smoke layer depth does not decrease to 0m. Actually, plot (c) (from Test 2) from the figure intentionally includes the spoiled readings that start around 900s. As it can be seen, the smoke layer depth value from the VFD system decreases, while, in fact, the smoke layer was deeper than at any other time in that experiment. For these situations, the input from an external system, like the OSID Array becomes necessary. An example of a VFD sensor being immersed in smoke is shown in Fig. 35, from camera 1 during Test 1.

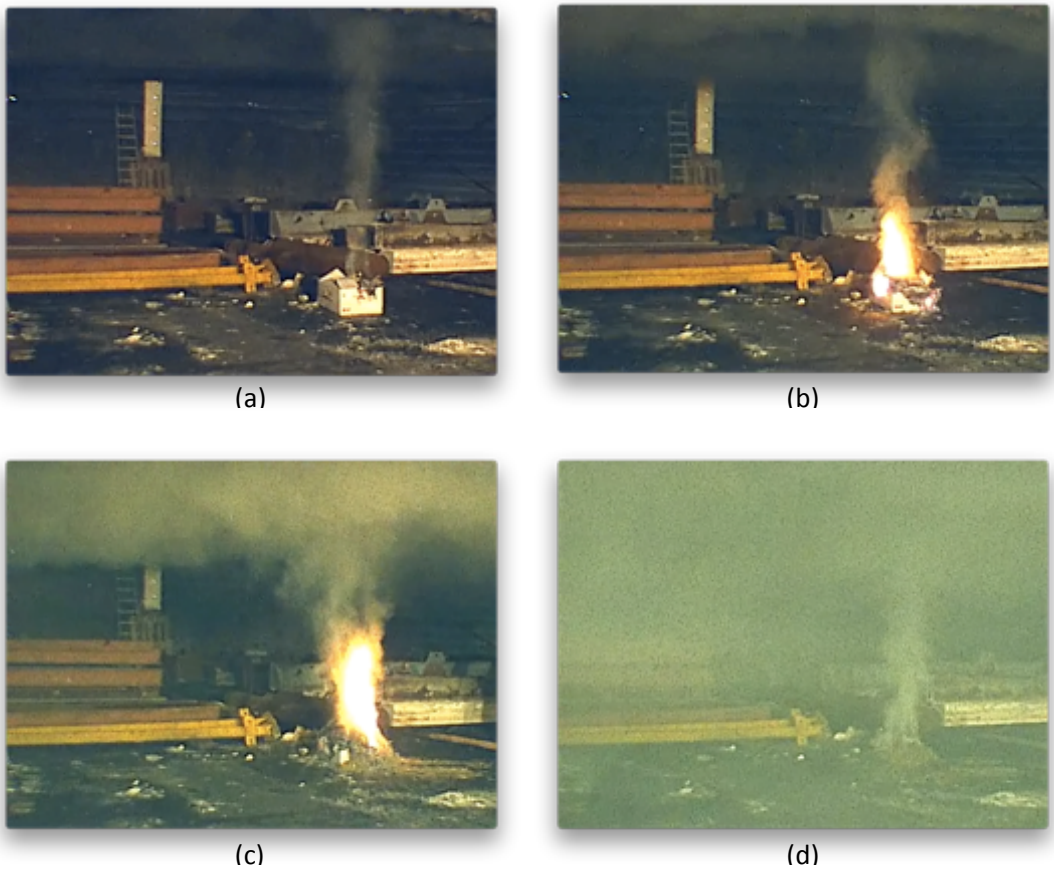

Figure 35: OSID-VFD smoke layer depth measurement experiments – Frames from Camera 1 during Test 1 after ignition at (a) 180 s, (b) 347 s, (c) 517 s, (d) 880 s

4.3 Further Approaches

The motivation of this thesis was the complementation of the VFD multi-view framework by combining it with volume sensors for the reduction of false alarms. The two OSID-based systems introduced throughout this document, i.e. the OSID 2-D Mesh and the OSID Array, were implemented and tested independently, showing an initial overall good response. Their immunity to the dust and steam that cause false alarms in VFD assumed correct based on the fabricant's reports. However, additional experiments with these nuisance sources would give valuable information to analyze the performance of the combined system. The implementation of the offline combination of VFD with OSID with real data (e.g. the data collected from the experiments) was out of the scope of this thesis. However, the output files from the OSID algorithms are available for the two sets of experiments. Therefore, the analysis of the combination of the systems is to be further done when the FireCube output is ready (for the first experiments).

The CSV file from the OSID Diagnostic Tool not only includes fire alarm information, but it also includes the attenuation values from both, the UV and the IR signal of each emitter as mentioned in Section 2.1.1. The initial approach presented in this thesis only used the alarm information as an input for the OSID algorithms. Nevertheless, the attenuation information could be further analyzed to create more elaborate decision algorithms. An example of such data is shown in Fig. 36, where the UV and IR attenuation values corresponding to the first of the A emitters in the 2-D Mesh of the first smoke detection and localization experiments are plotted.

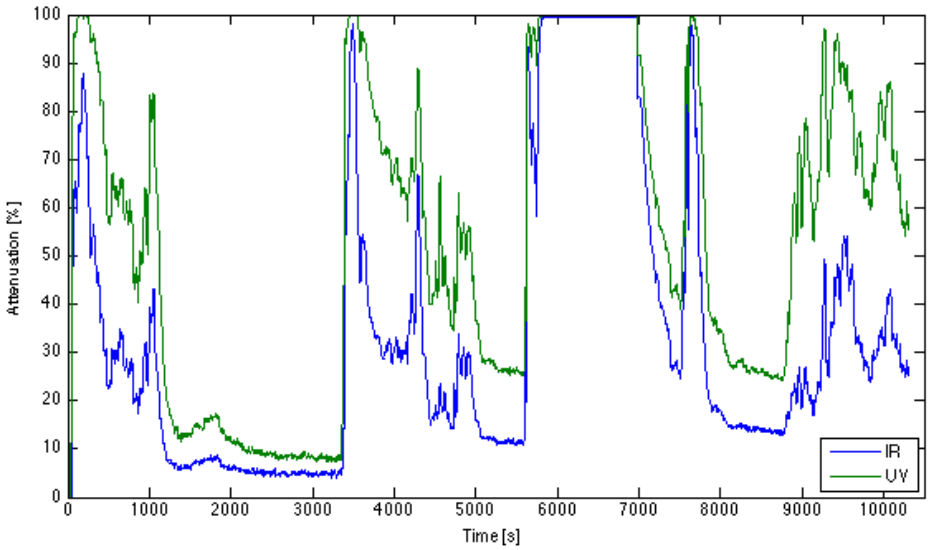

Figure 36: Smoke detection and localization first experiments – UV and IR attenuation readings of A_1

5. Conclusions

By the end of this thesis, two different systems based on volume sensors (OSID) were introduced. Also, two new algorithms in charge of the processing of the information gathered by the OSID-based systems were presented. The corresponding modifications of the existing FireCube VFD multi-view framework were also introduced and explained. After the work done, the systems and algorithms designed, and the experiments made, it can be concluded that:

- It was possible to use the readings from OSID detectors in the 2-dimensional system designed for the detection and localization of smoke, only at initial stages of the fire. This limitation is associated to the working principle of the OSID, which requires them to be installed in high locations, close to the ceiling. The buildup of the smoke layer gets the 2-dimensional OSID system (OSID 2-D Mesh) immersed in smoke and prevents it from doing further readings. A similar system with other types of sensors that did not require a high installation could overcome this limitation. The proposed algorithm and modification of the existing decision-making by the VFD multi-view algorithm would still be valid in such a system.
- It was also possible to use the OSID detectors in a linear system named the OSID Array, which was designed to retrieve the depth of the smoke layer. The sensitivity of the system, however, depends on the number of OSID emitters in the array (which is 7 per systems, although multiple systems could be installed in a series in case of a high construction).
- The modifications of the existing FireCube VFD multi-view framework theoretically reduce (given an correct input) the missed detections or false alarms due to illumination problems, steam or dust. An additional improvement on the VFD framework reduces the computational cost of the VFD algorithm based on the inputs from the volume sensors.
- The two sets of experiments performed with the two OSID systems designed showed that the systems worked with some limitations based on the coarseness of the 2-D Mesh, the number of emitters of the OSID Array, and physical parameters like the air velocities. The actual combination of the systems is yet to be done, based on the retrieval of detection data from the VFD multi-view framework for the smoke detection and localization experiments. Additional tests could also be done, exposing the combined system to the nuisance sources that cause malfunctioning of the VFD alone.

6. References

[1] Nelson, H.E., and F.W. Mowrer. "Emergency Movement." In *SFPE Handbook of Fire Protection Engineering*, by P.J. DiNenno, 3.367-3.380. Quincy, MA: NFPA, 2002.

[2] Schifiliti, R.P., B.J. Meacham, and R.L.P Custer. "Design of Detection Systems." In *SFPE Handbook of Fire Protection Engineering*, by P.J. DiNenno, 4.1-4.43. Quincy, MA: NFPA, 2002.

[3] Verstockt, S. *Multi-modal Video Analysis for Early Fire Detection.* Ghent: Ghent University, 2012.

[4] Cleary, T.G. "Video Detection and Monitoring of Smoke Conditions." Building and Fire Research Laboratory, NIST, Gaithersburg, MD.

[5] Elliott, B. "Performance Based Testing of Video Image Detection Devices." FM Approvals, Norwood, MA.

[6] Gottuk, D.T. "Video Image Detection Systems Installation Performance Criteria Research Project." Fire Protection Research Foundation, Quincy, MA, 2008.

[7] National Fire Protection Association. "Unwanted Fire Alarms." Quincy, MA, 2011.

[8] Dell'Orfano, M.E. "Analysis of False Alarms in Commercial Occupancies." South MEtro Fire Rescue Authority, Centennial, CO.

[9] Ahrens, M. "False Alarms and Unwanted Activations." National Fire Protection Association, Quincy, MA, 2004.

[10] Jahn, W. *Inverse Modeling to Forecast Enclosure Fire Dynamics.* Edinburgh: The University of edinburgh, 2010.

[11] Cleary, T. "Results From a Full-Scale Smoke Alarm Sensitivity Study." *13th annual Suppression and Detection Research & Applications Symposium (SUPDET 2009), .* Orlando, FL: Fire Protection Research Foundation, 2009.

[12] Milke, J.A., and T.J. McAvoy. "Analysis of Fire and Non Fire Signatures for Discriminating Fire Detection." *Fire Safety Science-Proceedings of the Fifth International Symposium.* 819-828.

[13] Jones, W.W. "An Algorithm for Fast and Reliable Fire Detection." *8th Fire Suppression & Detection Research Application Symposium.* Orlando, FL, 2004.

[14] Gottuk, D.T., M.J. Peatross, R.J. Robby, and C.L. Beyler. "Advanced Fire Detection Using Multi-Signature Alarm Algorithms." *Fire Safety Journal* 37 (2002): 381-394.

[15] Chena, S.J., D.C. Hovdeb, K.A. Petersona, and A.W. Marshall. "Fire Detection Using Smoke and Gas Sensors." *Fire Safety Journal* 42 (2007): 507-515.

[16] Heimann Sensor Technologies. *Thermopile Arrays and Imaging.* http://www.heimannsensor.com/products_imaging.php (accessed 04 15, 2013).

[17] Foote, M.C., et al. "Thermopile Detector Arrays for Space Science Applications." Jet Propulsion Laboratory, California Institute of Technology, Pasadena, CA.

[18] *LiDAR.* http://en.wikipedia.org/wiki/LIDAR (accessed 04 20, 2013).

[19] Belkhouche, Y., B. Buckles, and P. Duraisamy. "Registration of 3D-LiDAR Data with Visual Imagery Using Shape Matching." Department of Computer Science and Engineering, University of North Texas.

[20] Mastin, A., J. Kepner, and J. Fisher. *Automatic Registration of LIDAR and Optical Images for Urban Scenes.* Computer Science and Artificial Intelligence Laboratory, Massachusetts Institute of Technology, Cambridge, MA: IEEE, 2009.
[21] Knox, R. "Open-Area Smoke Imaging Detection (OSID)." XTralis Pty. Ltd., 2010.
[22] Xtralis AG. "OSID Smoke Detector Product Guide." 03 2011.
[23] Verstockt, S., et al. "FireCube: A Multi-View Localization Framework for 3D Fire Analysis." *Fire Safety Journal* 46 (2011): 262-275.
[24] McGrattan, K., and G. Forney. "Fire Dynamics Simulator (Version 4) User's Guide." Fire Research Division, National Institute of standards and Technology, 2006.
[25] Bathe, K.J., and H. Zhang. "A Mesh Adaptivity Procedure for CFD and Fluid-Structure Interactions." *Computers and Structures* 87 (2009): 604-617.
[26] Ghent University. *Car Park Fire Safety.* http://www.carparkfiresafety.be (accessed 04 25, 2013).